Ionoregulatory aspects of the hypoxia-induced osmorespiratory compromise in the euryhaline Atlantic killifish (*Fundulus heteroclitus*): the effects of salinity

Marina Giacomin[1,*], John O. Onukwufor[1,2], Patricia M. Schulte[1] and Chris M. Wood[1,3]

[1]Department of Zoology, The University of British Columbia, Vancouver, BC, Canada V6T 1Z4
[2]Department of Anesthesiology and Perioperative Medicine, University of Rochester Medical Center, Rochester, NY, USA 14642
[3]Department of Biology, McMaster University, Hamilton, ON, Canada L8S 4K1

*Corresponding Author's Current Address: Dr. Marina Giacomin. Biological Sciences Dept., University of Alberta, Edmonton, AB, Canada, TG6 2R3. Email: mussoigi@ualberta.ca - Tel: 1-604-868-0922

ORCID ID: Marina Giacomin 0000-0002-8163-3285
ORCID ID: John Onukwufor 0000-0003-4776-5003
ORCID ID: Patricia M. Schulte 0000-0002-5237-8836
ORCID ID: Chris M. Wood 0000-0002-9542-2219

Key Words: ion regulation, hypoxia, mummichog, trade-offs,

Summary statement: In the euryhaline killifish, ionoregulatory responses to acute hypoxia involve decreases in gill ion fluxes and permeability when in freshwater and seawater, but increases when in isosmotic salinity.

Abstract

The osmorespiratory compromise is a physiological trade-off between the characteristics of the gill that promote respiratory gas-exchange and those that limit passive fluxes of ions and water with the environment. In hypoxia, changes in gill blood flow patterns and functional surface area that increase gas transfer can promote an exacerbation in ion and water fluxes. Our goal was to determine whether the osmorespiratory compromise is flexible, depending on environmental salinity (fresh, isosmotic and sea water) and oxygen levels (hypoxia) in euryhaline killifish, *Fundulus heteroclitus*. Plasma ion concentrations were minimally affected by hypoxia, indicating a maintenance of osmoregulatory homeostasis. In FW-killifish, hypoxia exposure reduced branchial Na^+/K^+-ATPase and NEM-sensitive-ATPase activities, as well as diffusive water flux rates. Unidirectional Na^+ influx and Na^+ efflux decreased during hypoxia in FW, but net Na^+ flux remained unchanged. Net loss rates of Cl^-, K^+ and ammonia were also attenuated in hypoxia, suggesting both transcellular and paracellular reductions in permeability. These reductions appeared to be regulated phenomena as fluxes were restored immediately in normoxia. Na^+ flux rates increased during hypoxia in 11 ppt, but decreased in 35 ppt, the latter suggesting a similar response to hypoxia as in FW. In summary, FW- and SW-killifish experience a reduction in gill permeability, as seen in other hypoxia-tolerant species. Fish acclimated to isosmotic salinity increased Na^+ influx and efflux rates, as well as paracellular permeability in hypoxia, responses in accord with the predictions of the classic osmorespiratory compromise.

Introduction

The teleost fish gill is a multifunctional organ that is the primary site for ion and gas exchange in addition to playing a central role in acid-base balance and nitrogenous-waste excretion (Evans, 2005). When needed, branchial oxygen exchange can be improved by increasing water flow across the gills (ventilation) and also changing the rate and pattern of gill blood flow (perfusion) (Perry et al., 2009). A reduction in heart rate and increase in cardiac stroke volume, can lead to a recruitment of otherwise unperfused lamellae (Booth, 1978), thereby increasing the functional surface area and reducing the blood-to-water diffusion distance for oxygen. However, an exacerbation of the unfavourable ion and water fluxes can occur. As stated in the classic first paper on this topic (Randall et al., 1972) "*Any change in the pattern of blood and water flow which reduces diffusion distance or increases the functional exchange area between blood and water will increase the rate of ion and water diffusion, unless there are compensatory reductions in the permeability of the gill epithelium*". This functional trade-off in optimal gill function has been termed the osmorespiratory compromise (Randall et al., 1972; Gonzalez and McDonald, 1992).

To date, the osmorespiratory compromise has been relatively well characterized in response to exercise. In the highly aerobic freshwater rainbow trout (*Oncorhynchus mykiss*), increases in swimming activity led to elevations in ion and water fluxes (Wood and Randall, 1973a; Wood and Randall, 1973b; Wood and Randall, 1973c; Gonzalez and McDonald, 1992; Postlethwaite and McDonald, 1995; Onukwufor and Wood, 2018).

However fewer studies have looked at this phenomenon in response to the reduction of oxygen in the water. In hypoxia, fish improve the conditions for oxygen uptake by ventilating more water (Perry et al., 2009), and by changing blood flow patterns at the lamellae so as to increase functional surface area and decrease diffusion distance for exchange (Booth et al., 1978; Nilsson et al., 1995; Sundin and Nilsson, 1998). A likely consequence of these mechanisms is again a disturbance of ion and water balance as a result of the osmorespiratory compromise. Indeed, when exposed to hypoxia, rainbow trout experienced an increase in ion loss (Thomas et al., 1986; Iftikar et al., 2010; Robertson et al., 2015a), an effect that was paralleled by modifications in the gill epithelium, where ionocytes (mitochondria-rich cells) became more exposed, thereby increasing in surface area (Iftikar et al., 2010; Matey et al., 2011). In contrast, the Amazonian oscar (*Astronotus ocellatus*), a hypoxia-tolerant fish, exhibited a decrease in branchial ion and water fluxes in hypoxia (Wood et al., 2009; De Boeck et al., 2013; Robertson et al., 2015b). In addition, a reduction

in the exposed surface area of ionocytes, due to pavement cell modifications, was observed at the gills (Wood et al., 2009; Matey et al., 2011; De Boeck et al., 2013). These responses occurred despite the fact that the oscar increased ventilation and the O_2 transfer factor of the gills (an index of effective gill O_2 permeability) during hypoxia (Scott et al., 2008a; Wood et al., 2009). These data suggest that hypoxia tolerant fishes may circumvent or decouple the osmorespiratory compromise, by recruiting specific mechanisms at the level of the gill, preventing a disruption in the ionic balance, while gas exchange in hypoxia remains unnafected.

A few studies have examined the osmorespiratory compromise in SW (Sardella and Brauner, 2007). Fish in SW are hypoosmotic, contrary to what is seen in FW. Therefore, it has always been thought that fish would face a net ion loading and water loss during hypoxia and exercise, given the reversed nature of the ionic gradients between fish and environment (Gonzalez, 2011). The few experimental studies addressing the osmorespiratory compromise in seawater have supported this conclusion (Farmer and Beamish, 1969; Stevens, 1972; Wood et al., 2019). Additionally, there is no research of this phenomenon at the isosmotic salinity (the salinity at which the concentration gradient between the body fluids and external water is minimal). In theory, the osmorespiratory compromise at this salinity should be negligible, since no net movement of ions and water between the plasma and the environment should occur. A goal of the present study is to address these knowledge gaps.

Our overall goal was to increase our understanding of the ionoregulatory aspects of the osmorespiratory compromise during hypoxia across a range of salinities. We chose the Atlantic killifish, also known as mummichog, *Fundulus heteroclitus* as our model, due to its outstanding euryhalinity (Marshall, 2013) and its exceptional tolerance of hypoxia (Cochran and Burnett, 1996; Richards et al., 2008; McBryan et al., 2016). Killifish are native to estuaries and salt marshes while often enter rivers and creeks. In these environments, they can encounter variations in salinity and dissolved oxygen. In recent studies, we found that salinity affected killifish oxygen consumption and hypoxia tolerance (Giacomin et al., 2019) and also water exchange rates (Wood et al., 2019). Key findings from these two studies were that killifish increased gill ventilation during hypoxia, and exhibited the classic hypoxic bradycardia. Acclimation to FW led to reductions in hypoxia tolerance, likely due to a decrease in gill respiratory surface area and the presence of a greater interlamellar cell mass. Acclimation to 11 ppt (i.e. the isosmotic salinity for killifish) proved to be the most advantageous for respiratory gas exchange.

With this background in mind, our overall hypothesis was that there is a trade-off between efficient gas exchange and ion/water balance at the gills (osmorespiratory compromise) and the nature of this trade-off is flexible, depending on environmental salinity and oxygen levels. This hypothesis led to several predictions. Our first prediction was that killifish would reduce gill ion permeability in acute hypoxia, minimizing the fluxes of ions and water in both FW and SW, as seen in the other hypoxia-tolerant species. Secondly, we predicted that in FW and SW, killifish would decrease the exposed surface area of ionocytes when exposed to hypoxia, so that respiratory surface area could be maintained while the ion permeability was reduced, thereby avoiding the negative osmoregulatory effects of the osmorespiratory compromise. Lastly, we posited that in killifish acclimated to the isosmotic salinity, the effects of the osmorespiratory compromise would be minimal so that permeability could be increased without incurring negative osmoregulatory effects of the osmorespiratory compromise.

Material and Methods

Experimental animals

The experiments were performed throughout the year, from multiple field collections (April – October), between 2014 and 2018. All procedures were approved by the University of British Columbia Animal Care Committee (AUP A14-0251) and complied with the guidelines of the Canada Council for Animal Care. *Fundulus heteroclitus macrolepidotus* (northern subspecies) were collected by beach seine from a brackish estuary near Hampton, NH, USA by Aquatic Research Organisms (Inc.) and air-shipped to the University of British Columbia, where they were held initially in 20 ppt water, the same as used by the supplier. They were later directly transferred to their experimental salinities, and held there for at least 6 weeks in each salinity prior to experimentation. There were no mortalities. Fish were held in 120-L glass tanks, containing FW (0 ppt: recirculating, charcoal-filtered dechlorinated Vancouver tap water $[Na^+]$ = 0.09, $[Cl^-]$ = 0.10, $[Ca^{2+}]$ = 0.13, $[Mg^{2+}]$ = 0.01 mmol/L) or FW mixed with Instant Ocean Aquarium Salt (Instant Ocean, Spectrum Brands, Blacksburg, VA, USA) up to 11 ppt ($[Na^+]$ = 146, $[Cl^-]$ = 196, $[Ca^{2+}]$ = 4.3, $[Mg^{2+}]$ = 21.0 mmol/L) or SW (35 ppt: $[Na^+]$ = 459, $[Cl^-]$ = 663, $[Ca^{2+}]$ = 12.4, $[Mg^{2+}]$ = 53.6 mmol/L). Fish were fed daily with commercial flakes (Nutrafin Max Tropical Flakes) and fasted for at least 24 h prior to experiments. Salinity in the tanks and in the water prepared for experiments was monitored

with a conductivity meter (Cond 3310, WTW, Xylem Analytics, Weilhem, Germany). The photoperiod was 12-h light and 12-h dark, and the temperature during both acclimation and experimentation was 18 - 20ºC. Water PO_2 was monitored during acclimation and throughout all experiments using a handheld oxygen meter (Accumet AP84, Fisher Scientific, Toronto, ON, CA).

The influence of hypoxia and salinity on plasma ion composition and gill ionoregulatory enzymes

Fish (n = 8 at each salinity and O_2 level) were held in individual plastic containers whose sides were replaced with a plastic mesh for free water flow. These were placed in 30-L darkened Plexiglas tanks overnight, one for each acclimation salinity (FW, 11 ppt and SW). The water in each 30-L tank was aerated and continuously recirculated by a small submersible water pump. Approximately 80% of the water was replaced prior to the start of the trial to avoid nitrogenous-waste build-up. PO_2 was either maintained at normoxia (approximately 155 Torr = 20.7 kPa) or reduced from normoxia to hypoxia (15 ± 2 Torr, = 2 kPa) over a 30-min period and maintained at a constant level with bubbling of N_2 or air. Fish were kept in hypoxia for 3 h, and at the end of the experiment were immediately euthanized with an overdose of neutralized MS-222 (Syndel Laboratories, Nanaimo, B.C., Canada). Normoxic fish underwent the same protocol, but PO_2 was kept at normoxia. Blood samples (~100 µL) were quickly drawn by caudal puncture using a modified gas-tight Hamilton 100 µL-syringe (Reno, NV, USA). Two 5-µL micro-hematocrit tubes were filled with blood and centrifuged at 10000 *g* for 10 min. The remainder of the blood was also centrifuged (5 min, 10000 *g*), and the separated plasma was then flash-frozen in liquid N_2. Additionally, the left-hand side of the gill basket was excised and also flash-frozen in liquid N_2. Plasma and tissue samples were kept at -80ºC until analysis of plasma ion concentrations and osmolality, plasma lactate concentration, and gill Na^+/K^+ and H^+-ATPase activities (described below). The right-hand side of the gill basket was immediately fixed in Karnovsky's fixative for 24 h at 4ºC. The samples were transferred to 0.1 M sodium cacodylate and stored at 4°C until use. For scanning electron microscopy (SEM), sections of the center part of the second gill arch were progressively dehydrated in ethanol, critically point dried with CO_2, and then sputter-coated with 9 nm of gold-palladium. Samples were imaged on a Hitachi S-4700 Field Emission Scanning Electron Microscope (Tokyo, Japan) at 2000 x magnification.

The influence of hypoxia and salinity on diffusive water flux rates

Separate groups of fish (n = 12 at each salinity and O_2 level) were used to measure diffusive water fux rates in animals acclimated to FW, 11 ppt and SW, in normoxia and exposed to hypoxia. Groups of 6 fish were placed in darkened 1-L containers, at the acclimation salinity and dosed with 20 µCi/L of ^3H_2O (Amersham Pharmacia Biotech, Little Chalfont, UK). This loading period was performed overnight, while the chambers were constantly aerated, and temperature controlled to 20 ºC. Preliminary trials demonstrated that ^3H_2O concentration in the fish's body water pool and in the external water of the loading bath had reached an equilibrium within 6 h. After the loading period, the fish were quickly rinsed in non-radioactive water, and then transferred to individual darkened 250-mL containers, each filled with water at the appropriate salinity and PO_2, which served as the experimental chambers. Water PO_2 was set to normoxia (155 Torr) or hypoxia (15 ± 2 Torr) and was kept at these levels for the following 60 min. Water samples (5 mL) were taken every 5 min for 60 min. Normoxia was restored and a final water sample was taken at 8 h, a period when the radioactivity in the fish had completely equilibrated with the external water. Scintillation fluor (Optiphase, Perkin Elmer, Waltham, MA, USA) was added to the water samples in a 2:1 (fluor:water) ratio, and samples were stored in the dark for a minimum of 2 h to eliminate chemiluminescence prior to scintillation counting for beta emissions (Beckman Coulter, LS6500, Wellesley, MA, USA). Tests showed that quench was constant.

Diffusive water flux rates were calculated following methods described in Giacomin et al. (2017) and Onukwufor and Wood (2018). The rate of disappearance of ^3H_2O from the fish was calculated from the ^3H_2O washout from the animal as measured by its appearance in the water. The rate constant of ^3H_2O turnover (k: fraction of body water/h) was calculated as:

$$k = (\ln R_1 - \ln R_2) / (t_1 - t_2) \qquad \text{(Eq. 1)}$$

where R_1 and R_2 are total ^3H_2O radioactivities (cpm) in the fish (see below) at times t_1 and t_2 (h). Data were used only over the range where efflux was linear (up to 40 min from the start of experiment). The total volume of the system was estimated as the measured volume of external water (experimental container) plus the volume of the fish (assuming 1 g = 1 mL). The water sample that was taken at 8 h (after complete washout and equilibration had

occurred) plus all radioactivity removed by sampling during the experiment were used to calculate the total amount of ^3H_2O radioactivity that had been loaded into the fish (R_{total}). Therefore, the radioactivity remaining in the fish at each time interval (R_1, R_2, R_x) was then calculated by subtracting the ^3H_2O measured in the water from R_{total} at each time interval. The product of k x 100% has been reported as the percentage of the body water pool turned over per hour. This turnover can be converted to ml/g/h by multiplying by 0.80 ml/g, based on the estimates of Holmes and Donaldson (1969), Isaia (1984) and Olson (1992) that water comprises about 80% of body weight.

The influence of hypoxia and salinity on gill paracellular permeability and drinking rate

Separate groups of fish (n = 8 at each salinity and O_2 level) were used to measure gill paracellular permeability and drinking rate, using radiolabeled polyethylene glycol ([^{3}H]PEG-4000) following methods developed by Robertson and Wood (2014). Briefly, appearance of radioactivity in the carcass was used as a measurement of gill paracellular permeability, while appearance of radioactivity in the gut was used to measure drinking rate. Fish were exposed in groups of 8, for 3 h in 1 L of water at the acclimation salinity labeled with 25 µCi/L of [^{3}H]PEG-4000 (Amersham). Preliminary experiments demonstrated that there was no rectal excretion of [^{3}H]PEG-4000 in that time. Fish were allowed to settle in the aerated light-shielded experimental container for 2 h in normoxia prior to the addition of radioactivity. After that, PO_2 was either maintained at 155 Torr by air bubbling, or quickly reduced to 15 ± 2 Torr by N_2 bubbling, and when PO_2 reached hypoxic levels, the radioisotope was added. Water samples (5 mL) were taken at 0, 1.5, and 3 h for scintillation counting. At the end of 3 h, all fish were euthanized by an overdose of neutralized MS-222, rinsed in radioisotope-free water, blotted dry and kept on ice until dissection. The gastrointestinal tract was tied at both ends (to avoid content loss), and excised. The gut and remaining carcass were weighed separately, and digested in sealed vials with 2 N HNO_3 for 48 h at 60ºC, with periodic agitation. The digests were then centrifuged (5000 *g* for 5 min) and the clear supernatant was aliquoted for scintillation counting. Water and carcass digest samples (2 mL), and gut digest samples (0.2 mL) were dosed with 10 mL of scintillation cocktail (Ultima Gold AB; Perkin Elmer) and read on a scintillation counter (LS6500, Beckman Coulter). Radioactivity of the tissue digests was quench-corrected to the same counting efficiency as water samples based on a quench curve constructed previously with different amounts of tissue digest.

[^{3}H]PEG-4000 gill clearance rate (CR, µL/g/h) as a proxy for branchial paracellular permeability was calculated as follows:

[^{3}H]PEG-4000 CR = (cpm in carcass) / (mean water cpm/µL x W x T) (Eq. 2)

where cpm in carcass is the total amount of radioactivity in the carcass, W is the fish body mass (g) and T is time (h).

[^{3}H]PEG-4000 drinking rate (DR, µL/g/h) was calculated in a similar manner as follows:

[^{3}H]PEG-4000 DR = (cpm in gut) / (mean water cpm/µL x W x T) (Eq. 3)

where cpm in gut is the total amount of radioactivity in the gut.

Unidirectional and net ion flux rates in killifish acclimated to FW, 11 ppt and SW

Previous studies (Wood and Laurent, 2003; Wood, 2011) have demonstrated that it is necessary to use different methods to measure unidirectional fluxes of Na^{+} in saline waters versus FW, and we have adopted those methods in the present study. All techniques described below were employed to meet the experimental criteria outlined in Wood (2011). Briefly, the specific activity (SA: ratio of radioisotopic Na^{+} to "cold" Na^{+}) in the compartment where radioactivity appearance was being monitored, either water or fish, needs to remain less than 10% of the SA in the compartment to which radioactivity was added, so as to prevent the radio-isotopic back flux. The difficulty of meeting this criterion when measuring ^{22}Na fluxes in 11 and full strength SW have constrained our abilities to replicate at those salinities all the experiments performed in FW. A limitation of these approaches is that because the methods differ for influx and efflux determinations, and must be performed on different fish, over different time frames (0.5 h for influx, 3 h for efflux), influx and efflux rate measurements may not be quantitatively comparable to one another. Therefore comparisons should only be made of influx rates across treatments, and efflux rates across treatments, and not of efflux rates versus influx rates within treatments. Therefore, our investigation of the unidirectional ion flux responses to hypoxia is more detailed in FW than in 11 ppt or SW. Furthermore, our previous study (Giacomin et al., 2019) indicated that the impacts of the hypoxia-induced osmorespiratory compromise are most intense in FW-

killifish. All ^{22}Na measurements were made with a gamma counter (1470 Wallac-Wizard, Perkin Elmer, Waltham, MA, USA).

Separate groups of fish (n = 15 at each salinity and O_2 level) were used for each of the experimental series described below. For all experimental flux measurements, fish were held in individual 250-mL plastic containers, served with aeration tubing, darkened with black plastic and partially submerged in a wet table to ensure temperature control. The water surface was covered in plastic so to avoid oxygen diffusion from the air, and to prevent the fish from performing aquatic surface respiration.

Ion fluxes in FW-acclimated killifish

In FW, Na^+ influx (J^{Na+}_{influx}) was measured by monitoring the disappearance of radioactivity from the water. To that end, fish were transferred to the containers described above and allowed to acclimate overnight under flow-through conditions. Prior to the start of the experiment, flow-through ceased, water level was set at 250 mL, and 5 µCi ^{22}Na was added. Water samples (5 mL) were collected hourly for 3 h and stored for measurements of radioactivity, total Na^+, Cl^-, K^+ and ammonia concentrations.

At 3 h, the water was replaced with water that had been pre-equilibrated with N_2 to 15 ± 2 Torr (hypoxia) and dosed with the same amount of ^{22}Na. Water samples (5 mL) were collected again hourly for another 3 h. At the end of the hypoxia exposure time, the containers were quickly bubbled with air and normoxia was restored within 5 min. Recovery trials lasted for another 3 h. A control group (normoxia) was performed, where all the experimental procedures were conducted similarly, with the exception that the animals were maintained in normoxia throughout the whole 9-h duration of the trial. Fish were weighed at the end of the experiment. At each 1-h period, the unidirectional Na^+ influx rate (nmol/g/h) was calculated as:

$$J^{Na+}_{influx} = [(cpm_i - cpm_f) \times V] / (\text{mean } SA_{ext} \times T \times W) \qquad \text{(Eq. 4)}$$

where, cpm_i and cpm_f are the ^{22}Na counts per mL in the water at the start and end of each 1-h period respectively, V is the volume in each period (L), mean SA_{ext} is the mean external specific activity of Na^+ (cpm/nmol), T is time (h) and W is the body mass (g).

Na^+ net flux rates (nmol/g/h) were determined from the concentrations of total "cold" Na^+ in the water (nmol/L) and calculated using the following equation:

$J^{Na+}_{net\ flux} = [([Na^+]_i - [Na^+]_f) \times V] / (T \times W)$ (Eq. 5)

where $[Na^+]_i$ and $[Na^+]_f$ are the Na^+ concentration the water (nmol/L) at the start and end of each 1-h period respectively, V is the volume in each period (L), T is time (h) and W is the body mass (g).

Unidirectional Na^+ efflux rates (nmol/g/h) were calculated as follow:

$J^{Na+}_{efflux} = J^{Na+}_{net\ flux} - J^{Na+}_{influx}$ (Eq. 6)

where $J^{Na+}_{net\ flux}$ was calculated by equation 5 and J^{Na+}_{influx} by equation 4.

Cl^-, K^+, and total ammonia ($NH_3 + NH_4^+$) net flux rates (nmol/g/h) were determined from the concentrations in the water (nmol/L) and calculated using an equation analogous to equation 5.

Unidirectional Na^+ influx and effluxes in 11 ppt- and SW-acclimated killifish

Separate groups of fish (n = 15 at each O_2 and salinity level) were used to determine the influence of hypoxia on the unidirectional influx of Na^+ in killifish acclimated to 35 ppt or 11 ppt. Na influx (J^{Na+}_{influx}) was determined by monitoring the appearance of radioactivity in the fish. Note that Wood (2011) concluded that approximately 80-90% of Na^+ influx occurs across the gills, and 10-20% across the gut in seawater killifish; the dominance of the gills would be even greater at intermediate salinity where drinking rate is lower. In order to avoid radiotracer recycling and maintain the 10% SA criterion (see above), a flux period of 0.5 h was employed (Wood and Laurent, 2003; Wood, 2011). Fish were allowed to settle in the containers described above overnight under flow-through conditions, and water volume was set to 250 mL prior to the start of the experiment with normoxic (155 Torr) or hypoxic (15 ± 2 Torr) water. Fish were exposed to these conditions for 2.5 h in order to mimic the duration of the hypoxia exposure employed in fish acclimated to FW. At 2.5 h, 10 µCi ^{22}Na was added to the water. Water samples were taken and at the start and at the end of the 0.5-h flux period and stored for measurements of radioactivity and total Na^+ concentration. The fish were then rinsed in non-radioactive water of the appropriate salinity (11 or SW) for 1 min, euthanized in neutralized MS-222 (0.5 g/L), blotted dry, weighed and processed for

measurements of whole body radioactivity (^{22}Na). Unidirectional influx rates (nmol/g/h) were calculated as follows:

$$J^{Na+}_{influx} = \Sigma_{(cpm\ in\ fish)} / (mean\ SA_{ext} \times T \times W) \qquad (Eq.\ 7)$$

where $\Sigma_{(cpm\ in\ fish)}$ is the total ^{22}Na radioactivity in the fish (cpm), mean SA_{ext} is the mean external specific activity of Na^+ (cpm/nmol), T is time (h) and W is the body mass (g).

Separate groups of fish (n = 15 at each O_2 and salinity level), different from those used for influx, were used to determine the influence of hypoxia on the unidirectional efflux of Na^+ in killifish acclimated to 35 ppt or 11 ppt. Na^+ efflux (J^{Na+}_{efflux}) was determined by loading the fish with ^{22}Na, and then monitoring the appearance of radioactivity in the water. To load ^{22}Na in the fish, they were incubated overnight in batches of 8 in 80 µCi ^{22}Na/L at the salinity of acclimation, in a 1.5-L Erlenmeyer glass container. The loading chamber was aerated and shielded from light. Previous tests show that a minimum of 10 h was needed for complete equilibration between the fish and the external media. After incubation, fish were quickly rinsed in non-radioactive water, then transferred to the same experimental chambers as described above, each containing 250 mL of sea water at the appropriate salinity. Water samples were taken every 0.5 h for 1.5 h, and then either normoxic (155 Torr) or hypoxic (15 ± 2 Torr) water was used to replace the water in the chambers. The volume was again adjusted to 250 mL, and additional water samples were taken every 0.5 h for 3 h. This was done as to provide the fish with the same time frame of hypoxia exposure as described for fish acclimated to 0 ppt. At the end of the experiment, fish were rinsed in non-radioactive water for 1 min, euthanized in neutralized MS-222 (0.5 g/L), blotted dry, weighed and processed for measurements of whole body radioactivity (^{22}Na). Unidirectional efflux rates were calculated as follows (Wood and Laurent, 2003):

$$J^{Na+}_{efflux} = [(k \times \Sigma_Z \times F) / W] \qquad (Eq.\ 8)$$

where k is the rate constant of radioactivity lost (% exchangeable whole body Na^+ pool/h) by the fish per unit time, Σ_Z is the total internal Na^+ pool (nmol/g), F is the fractional labeling of that pool by the radioisotope and W is the body mass (g). Σ_Z and F were obtained from Wood and Laurent (2003). The total radioactivity appearance in the water, including that removed in water sampling, when added to the radioactivity measured in the fish carcass, yielded the

total radioactivity in the fish at the start of the experiment. The slope of the natural logarithm of the loss of this radioactivity versus time provides the rate constant (k) of radioactivity lost, and it was calculated using an equation analogous to Eq. 1. Only data obtained during the hypoxia period were used.

Ammonia net flux rate ($J^{amm}_{net\ flux}$: nmol/g/h) was determined from the measured total concentrations of ammonia (NH_3 and NH_4^+) in the water and calculated as described for the FW trials above. Net flux rates of Na^+, K^+, and Cl^- were not measured in 11 ppt and SW due to the background ionic concentrations being too high to reliably detect fish-induced changes.

Analytical techniques

Water Na^+ and K^+ concentrations (nmol/L), and plasma Na^+ concentrations (mmol/L) were determined by atomic absorption (1275 Atomic Absorption Spectrophotometer, Varian, Mulgrave, Victoria, Australia) using certified commercial standards (Fluka Analytical, Sigma-Aldrich, St. Louis, MO, USA). Plasma osmolality (mOsm/kg) was measured using a Wescor vapor pressure osmometer and standards (Wescor 5100C, Logan, UT, USA). Water (µmol/L) and plasma (mmol/L) Cl^- were determined colorimetrically using the mercury-thiocyanate method described by Zall et al. (1956). Ammonia concentration (µmol/L) in the water was measured using the colorimetric method of Verdouw et al. (1978).

Plasma lactate concentration (mmol/L) was determined as described by Bergmeyer (1983). Briefly, plasma samples were deproteinized with 8% perchloric acid, centrifuged briefly to precipitate proteins (8 min, 5000 *g*), and assayed in triplicate on a microplate spectrophotometer (SpectraMAX Plus; Molecular Devices, Menlo Park, CA, USA) with a reaction buffer solution (0.18 M glycine, 0.15 M hydrazine, 0.015 βNAD^+, 15 U/mL lactate dehydrogenase, pH 9.4). The reaction mixture was incubated for 60 minutes at 37ºC, and lactate concentration was determined against a standard curve.

Na^+/K^+-ATPase and NEM-sensitive -ATPase activities (µmol ADP/mg protein/h) were measured in gill tissues according to protocols described in McCormick (1993) and Lin and Randall (1993) respectively. Tissues were homogenized (1:10 w/v) in ice-cold buffer solution [50 mM imidazole, 125 mM sucrose and 5 mM EGTA (pH 7.3)], centrifuged (5000 *g*, 3 min, 4 °C), and supernatants kept on ice throughout the analysis. All samples were assayed within 2 h of thawing and homogenization. Ouabain (0.05 mM) was used as an inhibitor of Na^+/K^+-ATPase with sodium azide (NaN_3 – 5.15 mM) as inhibitor of ATP synthase. N-ethylmaleimide (NEM) at 1.03 mM was used as an inhibitor of H^+-ATPase. An

important caveat to note is that at this high concentration, NEM may not be a specific inhibitor of only v-type H^+-ATPase and might inhibit other ATPases (Forgac, 1989; Lin and Randall, 1993). For this reason, in accord with Tipsmark et al. (2004) we describe these results as NEM-sensitive -ATPase throughout; all the tissue samples were analyzed using the same method, so the comparisons between treatments remain valid. Activity was calculated by the difference between the amounts of adenosine diphosphate (ADP) produced in control and inhibited reactions. Absorbance was monitored at 10 s intervals over 5 min (25ºC) on the same microplate spectrophotometer. Protein concentration on homogenates was determined using the Bradford Reagent (Sigma Aldrich).

For the measurement of hematocrit, micro-hematocrit tubes (2 x 5 µL) were centrifuged (10000 *g*, 10 min) and hematocrit (HCT) was measured as the percentage of packed RBCs (%RBC) within the total blood volume.

Morphometric quantification of exposed ionocyte surface area and density (number of ionocytes per mm^2) was performed on randomly selected areas of the afferent surface of filaments near the respiratory lamellae. The individual exposed surface areas of approximately 50 ionocytes were measured over randomly selected areas of the epithelium for each fish at 2000 x magnification. The surface area of individual PVCs was also measured on randomly selected cells from each of five fish on the same micrographs. Microridge density on the surface of PVCs was calculated on 20 random cells from each of five fish as the total number of intercepts (for the whole cell) of microridge profiles on a lattice grid composed of 2.82 x 2.82 µm squares superimposed on the micrograph. This result (total number of intercepts per individual cell) was then divided by the individual PVC surface area (μm^2), yielding intercepts per μm^2 of PVC surface area The exposed ionocyte fractional surface area (FSA) was calculated by multiplying ionocyte surface area (μm^2/cell) by ionocyte density (cells/μm^2).

Statistical analyses

All data are shown as mean ± SEM (n = number of animals). Assumptions of parametric statistics (data normality and homogeneity of variances) were checked, and if not met, data were transformed using a log transformation. Data were analyzed using one-way ANOVA, two-way ANOVA, or repeated measures ANOVA as appropriate. Detailed results of the statistical tests and post-hoc analysis are shown in figure captions. When applied, one-way ANOVA was followed by a Tukey post hoc test. Two-way ANOVAs were followed by

a Bonferroni post-hoc test. Mean values were considered significantly different when $p < 0.05$.

Results

Plasma ions and enzyme activity

Salinity acclimation exerted a significant overall effect on plasma ions and osmolality (Fig. 1A,B,C). Under normoxia, plasma [Na^+] was significantly higher in SW- (~150 mmol/L) and than in FW-acclimated fish (~135 mmol/L) (Fig. 1A) Plasma Cl^- followed a similar trend, where 11 ppt-acclimated fish showed an intermediate value between FW- and SW-acclimated fish (~110 and ~140 mmol/L respectively; Fig. 1B). Neither plasma [Na^+] (Fig. 1A) nor plasma [Cl^-] (Fig. 1B) was significantly affected by hypoxia at any salinity. There was no significant interaction between salinity and oxygen for plasma [Na^+] and [Cl^-] (Fig. 1A,B). Plasma osmolality was similar in fish acclimated to 11 and 35 ppt (~ 375 mOsm/kg) and both were significantly higher than FW-fish (~ 340 mOsm/kg; Fig. 1C). There was no significant effect of hypoxia and no significant interaction between oxygen and salinity on plasma osmolality (Fig. 1C).

Hypoxia exposure had a significant overall effect on both gill Na^+/K^+- and NEM-sensitive -ATPase activities, with activities being lower in hypoxia than normoxia (Fig. 2A,B). Two-way ANOVA did not detect a significant effect of salinity acclimation on either Na^+/K^+or NEM-sensitive -ATPase activity, and there was no significant interaction between salinity and oxygen.

Blood hematocrit and plasma lactate

Hypoxia exposure had a significant overall effect on blood HCT, while salinity acclimation did not (Fig. 3A). At all salinities, hypoxia exposure caused an increase in blood HCT, which was significantly different than normoxic values at 11 and 35 ppt (Fig. 3A).

There were significant overall effects of both salinity and hypoxia on plasma lactate concentration (Fig. 3B), however plasma lactate was significantly elevated only in FW and 11 ppt fish. Fish in 11 ppt showed the largest difference in plasma lactate between normoxia and hypoxia exposure (60% increase), followed by fish acclimated to FW (46% increase; Fig. 3B).

Diffusive water flux rates, gill paracellular permeability and drinking rate

Salinity acclimation had a significant overall effect on the diffusive water flux rate (Fig. 4A). Water flux rate was the highest (~94% of the body water pool/h) in fish acclimated to FW, and significantly different from fish acclimated to 11 ppt and SW, which had similar rates (~57 - 47%/h; Fig. 4A). There was a significant decrease (30%) with hypoxia exposure in FW-fish, but no effect of hypoxia in fish acclimated to 11 ppt and SW (Fig. 4A).

There was an overall effect of salinity on gill clearance rates of [^{3}H]PEG-4000, an index of gill paracellular permeability, while under normoxia, FW- and SW-fish exhibited very similar rates and 11 ppt-acclimated fish had a significantly lower rate (~ 1.0 µL/g/h) (Fig. 4B). While hypoxia exposure did not have an overall effect on the [^{3}H]PEG-4000 gill clearance rate (Fig. 4B), at 11 ppt gill clearance rate was elevated (Fig. 4B).

Both salinity acclimation and hypoxia exposure had significant overall effects on drinking rate (Fig. 4C). Under normoxia, drinking rate was the lowest in FW (~ 0.15 µL/g/h), and approximately 40-fold higher (~ 6.1 µL/g/h) in SW (Fig. 4C). Drinking rate was decreased significantly with hypoxia exposure (88%) at 35 ppt (Fig. 4C).

Unidirectional flux rates of Na^+, and net flux rates of Cl^-, K^+, and ammonia

In FW, there were no significant changes in unidirectional flux rates of Na^+ or the net flux rates of Cl^-, K^+, and ammonia in the fish subjected to the normoxic control sham procedures (data not shown). FW-killifish exhibited an average J^{Na+}_{influx} of 310 nmol/g/h in normoxia (Fig. 5A). In the first hour of hypoxia, J^{Na+}_{influx} did not change, but it decreased significantly by about 55% for the remainder of the hypoxia exposure (Fig. 5A). J^{Na+}_{influx} returned to pre-exposure levels as soon as fish were returned to normoxia (Fig. 5A). J^{Na+}_{efflux} showed a similar response pattern as seen for the influx, with an overall reduction in the second and third hours of hypoxia, with recovery back close to control levels upon re-instatement of normoxia (Fig. 5B). In normoxia, the average J^{Na+}_{efflux} was about -300 nmol/g/h, and during hypoxia, it decreased significantly by 50% at the second hour,and by 36% at the third hour (Fig. 5B). The resulting net flux rates (~ -25 nmol/g/h) were therefore essentially unchanged with no significant differences among normoxia, hypoxia, and recovery(Fig. 5C)

In normoxia, the average net Cl^- flux rate was -39 nmol/g/h, and did not change in the first hour of hypoxia, but was significantly reversed to about +100 nmol/g/h in the second and

third hours (Fig. 6A). Cl^- net flux rates returned to pre-exposure levels once normoxia was restored. In normoxia, the net K^+ flux rate was about -20 nmol/g/h and during hypoxia, it followed the same pattern as seen for unidirectional Na^+ fluxes, and net Cl^- fluxes, where the rates were unchanged in the first hour, but decreased substantially (by about 70%) in the second and third hours (Fig. 6B). In recovery, the K^+ flux rate was restored to levels similar to the original ones in normoxia (Fig. 6B). The ammonia excretion rate was about -350 nmol/g/h in normoxia, and it significantly decreased by about 60% immediately upon hypoxia exposure (Fig. 6C). Ammonia excretion did not change during subsequent hypoxia, but increased immediately back to control levels once normoxia was restored (Fig. 6C).

In SW, only single values were obtained for unirectional Na^+ flux rates during normoxia and hypoxia, and net flux rates of Na^+, K^+, and Cl^- were not measured. In Fig. 7, we have shown the overall time-averaged unidirectional Na^+ flux rates for normoxia and hypoxia of FW-killifish (from Fig. 5A,B) in order to make comparisons with fish acclimated to 11 ppt and SW. Note that the scale is broken to accommodate the wide range of values.

On average, J^{Na+}_{influx} in FW-fish was +310 nmol/g/h while in hypoxia this decreased to +210 nmol/g/h (Fig. 7A). The average J^{Na+}_{efflux} was -300 nmol/g/h while in hypoxia it decreased to -250 nmol/g/h (Fig. 7B). Fish acclimated to 11 ppt in normoxia showed a many-fold higher J^{Na+}_{influx} of +6400 nmol/g/h while in hypoxia this increased by 150% to +16000 nmol/g/h (Fig. 7A). There was also a 92% increase in J^{Na+}_{efflux} in 11 ppt fish exposed to hypoxia (-5400 nmol/g/h) in comparison to normoxia (-2800 nmol/g/h; Fig. 7B). The J^{Na+}_{influx} in normoxia of SW-acclimated fish was about +22000 nmol/g/h, which decreased significantly by 13% when fish were exposed to hypoxia (Fig. 7A). In normoxia, J^{Na+}_{efflux} was approximately -12000 nmol/g/h, and when SW-fish were exposed to hypoxia, it was not significantly different at about -10000 nmol/g/h (Fig. 7B). Although the absolute unidirectional Na^+ flux rates in SW were more than an order of magnitude higher than in fish acclimated to FW, the overall patterns of response to hypoxia were similar to those in fish acclimated to FW (Fig. 7). However, the patterns were different from those in fish acclimated to the isosmotic salinity (11 ppt), where fluxes increased rather than decreased during hypoxia. Note that the discrepancies in absolute values between unidirectional Na^+ influx and efflux rates in 11 ppt and 35 ppt fish (Fig. 7A,B) were likely of technical origin (see Methods), but the relative differences between normoxia and hypoxia remain comparable as they were determined by the same techniques within a salinity.

Salinity acclimation had a significant overall effect on $J^{amm}_{net\ flux}$, with elevated rates in both normoxia and hypoxia at 11 ppt relative to FW (Fig. 8). Hypoxia also had a significant overall effect, reducing rates at all salinities by 33-54%.

Gill epithelial morphology and morphometrics

Salinity acclimation had a significant effect on the exposed surface area of individual ionocytes while hypoxia exposure had no overall effect (Fig. 10A). The shape of ionocyte apical openings varied greatly among salinities. Fish acclimated to FW showed ionocytes that were circular, oval, triangular and roughly trapezoidal, with large exposed surfaces (Fig. 9A), compared to fish acclimated to 11 ppt and SW which showed much smaller round and/or oval apical openings (Fig. 9B,C). The surfaces also varied between showing protruding and flat microvilli. These were smaller in fish acclimated to 35 ppt (Fig. 9C). Hypoxia-exposed fish (Fig. 9D,E,F) had PVCs which were less complex in surface, with less developed microridges and flatter surfaces throughout. In FW, ionocyte surface area was higher than in SW, while at 11 ppt, fish exhibited intermediate-sized ionocytes (Fig. 10A). At 11 ppt, ionocyte surface area was significantly elevated in hypoxia. Both hypoxia and salinity had significant effects on individual PVC surface area (Fig. 10B). PVC surface area was significantly higher in hypoxia at 0 and 35 ppt, while no effects of hypoxia were seen at 11 ppt (Fig. 10B). Ionocyte density was significantly affected by salinity, where FW-fish had higher density than SW-fish. There was no significant effect of hypoxia on ionocyte density (Fig. 10C). PVC microridge density was significantly affected by hypoxia, independent of salinity acclimation (Fig. 10D). In fish exposed to hypoxia, microridge density (intercepts per unit surface area) decreased by 42% in FW-fish, and by 23% in 11 ppt- acclimated fish (Fig. 10D). There was a significant effect of salinity on ionocyte fractional surface area, where FW-fish had higher FSA than 11 ppt- or SW-fish (Fig. 10E).

Discussion

Overview

Overall, our findings lend support to our hypothesis that in the killifish there is a trade-off between efficient gas exchange and ion/water balance at the gills (osmorespiratory compromise) and the nature of this trade-off is flexible, depending on environmental salinity and oxygen levels. The gas exchange components of this tradeoff have been addressed in Giacomin et al. (2019), and the ion and water exchange components in the present investigation. This hypothesis led to several predictions with respect to osmoregulation. Our first prediction, that killifish would decrease gill permeability during hypoxia exposure, reducing ion and water fluxes in both FW and SW was generally supported. In FW-fish, active Na^+ influx rate, gill Na^+/K^+-ATPase and NEM-sensitive -ATPase activities (see Methods), ammonia, K^+ and Cl^- efflux rates, as well as diffusive water flux rates were all reduced in hypoxia. The responses of this suite of markers suggests that both transcellular and paracellular permeability were reduced during hypoxia as part of a regulated process. In SW, where Na^+ gradients are reversed, and Na^+ fluxes are complicated by the presence of a large exchange diffusion component, both Na^+ influx and efflux declined in accord with our prediction.

Contrary to our second prediction, in FW and SW, killifish did not decrease the exposed surface area of ionocytes when exposed to hypoxia, but increase the surface area of PVCs. Nevertheless, at 11 ppt, killifish significantly elevated the surface area of individual ionocytes, in accord with the increased flux rates at this salinity.

Our third prediction was that because killifish acclimated to the isosmotic salinity (11 ppt) were able to prioritize gas exchange during hypoxia, as shown by Giacomin et al., (2019), they would increase permeability while exhibiting minimal disturbances of ionoregulatory homeostasis. Both unidirectional Na^+ influx and efflux rates increased as well as [^{3}H]PEG-4000 clearance rate, in accord with our hypothesis. However, diffusive water flux rate was not altered by hypoxia. At all three salinities, plasma ions and osmolality were unaffected by hypoxia exposure, indicating that despite disturbances seen in ion and water fluxes, *F. heteroclitus* are able to maintain osmoregulatory homeostasis under hypoxia in diverse environments, via a flexible strategy with respect to the osmorespiratory compromise.

The effects of salinity and hypoxia on plasma ion homeostasis

Salinity acclimation had only a small effect on the plasma concentrations of Na^+, Cl^- and osmolality (Fig. 1), in accord with previous studies (Wood and Marshall, 1994). In their natural habitat, *F. heteroclitus* can encounter transient as well as seasonal fluctuations in salinity, therefore the ability to maintain ionoregulatory homeostasis is likely an adaptation for this unpredictable environment. As a result of this flexible strategy with respect to the osmorespiratory compromise, plasma ion concentration and osmolality were not significantly affected by hypoxia in killifish at any of the three salinities tested (Fig. 1), indicating a remarkable homeostatic regulation of these parameters, despite diverse changes in associated parameters such as flux rates and transport enzyme activities. In previous studies, an increase in plasma [Na^+] with hypoxia was observed for two contrasting species, the hypoxia-tolerant Amazonian oscar (*Astronotus ocellatus*) (Wood et al., 2007), and the hypoxia-intolerant rainbow trout (*Oncorhynchus mykiss*) (Thomas et al., 1986). In both studies, the slight increase in plasma [Na^+] was attributed to a fluid shift towards the intracellular compartment as well as a movement of Na^+ to balance the increased lactate in the plasma (Thomas et al., 1986). In our study, we observed an increase in plasma lactate concentration in response to hypoxia in FW and 11 ppt acclimated fish (Fig. 3B). Normoxic plasma lactate values at all salinities are comparable to previous studies in *F. heteroclitus* that employed similar blood-sampling techniques (Richards et al., 2008; Healy and Schulte, 2012). However they are above resting values reported for other larger fish where blood sampling by indwelling cathethers was possible (e.g. Milligan and Wood, 1986). Although blood acid-base status was not measured in the present study, Giacomin et al. (2019) reported that a comparable hypoxia exposure caused a reduction in blood pH. Therefore it is likely that killifish are able to deal with a hypoxia-induced acidosis by employing mechanisms that are independent of the modulation of plasma ions.

The effects of salinity and hypoxia on branchial enzyme activities

A fundamental problem imposed by hypoxia exposure is the maintenance of metabolic energy balance, as a decrease in blood O_2 content directly impacts mitochondrial energy production in the form of ATP (Boutilier and St-Pierre, 2000). Hochachka et al. (1996) suggested that maintaining transmembrane electrical gradients through Na^+/K^+-ATPase is amongst the most energetically costly processes performed by a cell. Using an

isolated gill perfusion preparation, Morgan and Iwama (1999) found that Na^+/K^+- and H^+-ATPase contributed to 35% of the total gill MO_2. Therefore, the reduction in both of these enzymes in FW fish exposed to hypoxia (Fig. 2A,B) was in accord with the reduction of actve Na^+ influx (Fig. 5A) and would have a clear benefit in terms of energy conservation. A similar rapid (3 - 4 h) down-regulation of Na^+/K^+-ATPase activity was observed in the Amazonian Oscar, where a lack of change in protein abundance raised the hypothesis that post-translational modifications may have been responsible for the reduction in enzyme activity (Richards et al., 2007; Wood et al., 2007). Notably killifish at 11 ppt and SW did not show this response.

FW-acclimated killifish have a reduced respiratory capacity in hypoxia relative to other salinities (Giacomin et al., 2019), which could account for the different strategy that they employed in dealing with the osmorespiratory compromise. We suggest that the downregulation in enzyme activities in the FW killifish could be a reflection of the compromised respiratory ability in these animals, as a strategy to conserve energy, possibly in concert with a simultaneous downregulation of gill permeability. This way, plasma ion concentrations were maintained and whole-animal ion balance remained unaffected, in accord with our overall hypothesis of flexible responses dependent upon salinity.

The effects of salinity and hypoxia on diffusive water flux rates, paracellular permeability and drinking rates

In confirmation of our initial prediction that killifish would decrease gill ion and water permeability when exposed to hypoxia, we observed a reduction in the flux of ^3H_2O across the gills, but this effect was salinity-dependent, occurring only in FW (Fig. 4A). ^3H_2O fluxes represent unidirectional diffusive water fluxes, and are approximately 100-fold larger than osmotic water fluxes, which are net water fluxes usually estimated from body weight changes and urine flow (Stevens, 1972; Isaia, 1984). Diffusive water fluxes are thought to occur mainly by the transcellular route (Evans, 1969; Isaia, 1984), very likely through aquaporins (Evans et al. 2005), whereas osmotic water fluxes may occur by both paracellular and transcellular routes. Additional explanation of the significance of diffusive water flux measurements has been provided by Onukwufor and Wood (2018) and Wood et al. (2019). In general, SW teleosts have lower gill permeability to water than FW teleosts (Evans, 1969), and the water permeability of euryhaline fishes decreases with transfer to SW (Potts and Fleming, 1970). This appears to correlate with lower expression of levels of aquaporins at

higher salinities (reviewed by Cutler et al., 2007; Madsen et al., 2015; Breves et al., 2016). Our data agrees with this, where in normoxia, fish that were acclimated to FW showed higher water permeability than their SW-acclimated counterparts.. The decrease in diffusive water flux in FW during hypoxia but not at the other salinities may suggest the involvement of aquaporins in this response.

Our findings of reduced diffusive water flux during hypoxia in FW killifish are comparable to observations on the Amazonian oscar, which was able to reduce both diffusive and osmotic water fluxes during hypoxia (Wood et al., 2009), while maintaining high branchial oxygen permeability (Scott et al., 2008a). The explanation offered by these authors was that there was an adaptive reduction in transcellular permeability, due to an observed paving over of ionocytes by pavement cells (PVCs), in addition to channel (e.g. aquaporin) closure (Wood et al., 2009; Matey et al., 2011). Thus, we speculate that this ability to similarly downregulate gill water permeability in the FW-acclimated killifish, an effective decoupling of the classic osmorespiratory compromise, could be an adaptation to frequent variations in O_2 in their natural enviroments (Layman et al., 2000; Smith and Able, 2003). In contrast, gill permeability and consequently diffusive water flux rates increased markedly in both goldfish (*Carassius auratus*) and rainbow trout during exposure to moderate hypoxia - the classic tradeoff of the osmorespiratory compromise response (Loretz, 1979; Onukwufor and Wood, 2018). When rainbow trout were exposed to continuing severe hypoxia, water flux rates returned to control levels, indicating some regulatory ability, perhaps involving aquaporins (Onukwufor and Wood, 2018).

[^{3}H]PEG-4000 (MW-4000) is a classic gill paracellular marker (Wood and Part, 1997) and its use in whole animal experiments in the influx direction has been validated (Robertson and Wood, 2014). In normoxia, 11 ppt fish had lower gill paracellular permeability, in par with the theory that at the isosmotic salinity, the need for active Na^+ excretion would be reduced, as gradients between fish and environment are minimal, and maintainance of high paracellular permeability unecessary (Wood and Marshall, 1994). Paracellular permeability increased in killifish acclimated to the isosmotic medium, opposite to what was seen in fish acclimated to FW and SW (Fig. 4B). These results coupled with increased ionocyte surface area at 11 ppt (Fig. 10A), may account for the elevation in unidirectional Na^+ fluxes (Fig. 7A,B), suggesting that despite the maintenance in respiratory gas exchange (Giacomin et al., 2019), no compromise in ion and osmoregulation occurred.

In hypoxia, no change in [^{3}H]PEG-4000 clearance rate was seen for the Amazonian oscar, and all reductions in gill permeability during hypoxia appeared to be transcellular in nature (Wood et al., 2009), contrary to our data (Fig. 4B). Noteworthy, the absolute branchial clearance rate in the FW oscar was less than 50% of that of the killifish in FW or SW. This suggests that the oscar may more tightly regulate gill permeabilty in its ion-poor environment, while the FW killifish with normally higher paracellular permeability may employ reductions in both paracellular and transcellular permeability during hypoxia as part of its flexible osmorespiratory strategy (discussed below).

Drinking rates in SW were much higher than in FW (Fig. 4C), in accord with several previous studies on *F. heteroclitus* (Potts and Evans, 1967; Scott et al., 2006; Wood et al., 2019), reflecting the fact that marine teleosts must ingest water to compensate for net osmotic water losses across the gills (Takei and Balment, 2009). SW-killifish reduced drinking in hypoxia, indicating that dealing with the absorption and excretion of excess salts gained upon imbibing SW must be an energy demanding process. In normoxia, the stimulation of drinking in SW and its cessation in FW are both thought to be mediated by the renin-angiotensin system (Malvin et al., 1980). Possibly the reduction of drinking in hypoxia is also mediated by the same pathway; further studies on this present an interesting area for future investigations.

The effects of salinity and hypoxia on ammonia excretion

Ammonia net flux rates were inhibited by hypoxia at all three salinities (Fig. 8). In FW, ammonia net fluxes decreased immediately upon hypoxia exposure (Fig. 6C). It is widely accepted now that in FW fishes the majority of ammonia excretion occurs transcellularly, most likely via Rh proteins (Wright and Wood, 2009; Weihrauch et al., 2009). Therefore, the reduction in net ammonia flux is likely another indication of a reduction in transcellular permeability in response to hypoxia exposure in FW-killifish. In addition to transcellular ammonia transport, paracellular ammonia flux is also probably an important pathway in SW-fishes, given the leakier nature of junctions in SW gills (Wilkie, 1997; Wilkie, 2002). Giacomin et al. (2019) have shown that at low PO_2s, *F. heteroclitus* depresses $\dot{M}O_2$ regardless of salinity acclimation, and therefore a reduction in aerobic metabolism could be an additional cause of decreased ammonia excretion.

The effects of salinity and hypoxia on unidirectional and net ionic flux rates

Fish that were acclimated to 11 ppt or SW had more than one order of magnitude higher fluxes than in FW-fish (Fig. 7A), in agreement with previous studies (Motais et al., 1966; Potts and Evans, 1967; Maetz et al., 1967; Wood and Laurent, 2003; Wood, 2011). Fluxes in 11 ppt were 20-fold higher than FW, but 3.5-fold lower than in SW (Fig. 7A). This is explained by the fact, that in contrast to FW-acclimation, at higher salinities, killifish exhibit a large percentage contribution of exchange diffusion to unidirectional Na^+ fluxes (reviewed by Wood and Marshall, 1994). This component is proportional to external [Na^+] (Wood and Marshall, 1994), and not present in FW-animals (Patrick et al., 1997).

In our previous work (Giacomin et al 2019), we showed that in comparison with SW- and 11 ppt-acclimated fish, FW-acclimated animals showed the grestest limitation in respiratory capacity when exposed to hypoxia. Therefore, we expected that the largest compensatory responses in order to maintain ionoregulatory balance would be seen in FW-fish. Based on the responses of the Amazonian oscar (Wood et al., 2007; Wood et al., 2009; DeBoeck et al., 2013;Robertson et al., 2015a), we had predicted that the killifish would show a hypoxia response opposite to the classic osmorespiratory compromise in both FW and SW, decreasing overall gill permeability and the fluxes of ions. Indeed, the FW-acclimated *F. heteroclitus* reduced both J^{Na+}_{influx} and J^{Na+}_{efflux} during hypoxia, so that no changes were seen in net fluxes (Fig. 5C). Given the lack of an exchange diffusion component in the FW-killifish (Patrick et al., 1997), the very similar reductions of J^{Na+}_{influx} and J^{Na+}_{efflux} during hypoxia were probably independent of each other. The reductions in both unidirectional fluxes appear to be regulated phenomena, since they were significantly inhibited only at the second hour of exposure, remaining depressed until normoxia was restored (Fig. 5A). This represents an effective decoupling of the classic osmorespiratory compromise as part of the flexible strategy. Interestingly, net K^+ flux was reduced with an identical time-dependent profile (Fig. 6B). As K^+ concentrations are much higher inside cells than in blood plasma, K^+ flux is often considered a marker of transcellular permeability (Laurén and McDonald, 1985; Wood et al., 2007; Wood et al., 2009; Robertson et al., 2015b), so a role for the transcellular pathway in Na^+ flux reduction is implicated, as in the oscar (Wood et al., 2009). This would also be in accord with the transcellular origins of the reductions in diffusive water permeability and ammonia excretion (Fig. 6C), both discussed earlier.

FW-killifish do not take up Cl^- at the gills (Patrick et al., 1997; Patrick and Wood, 1999; Wood, 2011), only at the opercular epithelium (Wood and Laurent, 2003), so the apparent reversal of net Cl^- loss during hypoxia (Fig. 6A) suggests that that the diffusive loss pathway at the gills for Cl^- was also down-regulated. However, it should be noted that none of the positive values values of Cl^- flux during hypoxia (Fig. 6A) were significantly different from zero (one sample t-test). Altogether, our results for *F. heteroclitus* point to a response different from the typical osmorespiratory compromise seen in salmonids, where ion and water fluxes are exacerbated when gas transfer needs to be upregulated (Wood and Randall, 1973b; Wood and Randall, 1973c; Iftikar et al., 2010).

We earlier showed that acclimation to 35 ppt also placed constraints on respiratory performance during hypoxia, though not as severe as those at 0 ppt (Giacomin et al., 2019). At 35 ppt, fish are hypoosmotic, so the classical osmorespiratory compromise would predict increased Na^+ loading. This did not occur - both Na^+ influx and efflux rates were reduced in hypoxia by about 15%, though only the change in the former was significant, and there was no significant change in the [^{3}H]PEG-4000 clearance rate. While the Na^+ efflux component includes the active pathway through leaky paracellular junctions (Evans, 2005; Evans, 2008), it must be remembered that the major components of both unidirectional Na^+ fluxes are exchange diffusion fluxes (Motais et al., 1966; Potts and Evans, 1967; Maetz et al., 1967; Wood and Marshall, 1994). Overall, these observations suggest that there was a decrease in branchial permeability during hypoxia in SW, as in FW, again providing evidence for a flexible responste, that is salinity dependent. Wood and Grosell (2015) have reported that acute hypoxia exposure reduced branchial transepithelial potential (TEP) in *F. heteroclitus* acclimated to both 0 and 35 ppt, providing additional evidence of decreased ion fluxes at both salinities.

Killifish acclimated to isosmotic salinity (11 ppt) have the greatest capacity to maintain oxygen consumption in hypoxia (Giacomin et al., 2019), in accord with the idea that the osmorespiratory compromise at the isosmotic salinity is of minimal consequence. The observed increases in both Na^+ influx and efflux rates coupled with the increase in the paracellular permeability likely reflected an increase in functional surface area of the gills for respiratory gas exchange. Additionally, we observed an increase in the exposure of ionocytes in hypoxia. On the other hand, the unchanged diffusive water flux rate (Fig. 4A), and the greatest lactate accumulation (Fig. 3B) at this salinity argue against our prediction. Unfortunately, no data are available for TEP in 11 ppt-acclimated fish exposed to hypoxia,

which might clarify the responses seen. Perhaps there are other constraints on gill function at the isosmotic salinity of which we are currently unaware.

Salinity and hypoxia-induced changes in gill morphology

We observed a well established effect of salinity on ionocyte surface area (Fig. 10A), where FW-fish showed large, oval and sometimes trapezoid shaped ionocytes (Fig 9A), with protruding microvilli, whereas SW-fish had ionocytes with small round deep openings, called apical crypts (Fig 9C). These salinity-specific differences in ionocyte morphology are in accordance with previous studies on FW and SW-acclimated killifish, where morphological differences were similarly noted (Katoh and Kaneko, 2002; Katoh and Kaneko, 2003; Scott et al., 2008b).

Rainbow trout increase the density and exposed surface area of ionocytes shortly after hypoxia exposure (Iftikar et al., 2010; Matey et al., 2011), in accord with the typical osmorespiratory compromise (increased Na^+ flux rates) shown by this species. In the Amazonian oscar, large reductions in Na^+ flux rates during hypoxia were paralleled by an 80% reduction in fractional ionocyte surface area which was largely due to covering by PVCs (Wood et al., 2009). A simultaneous increase in functional gill surface area (due to increased perfusion) and decrease in exposed ionocyte surface area, was believed to maintain O_2 transfer in hypoxia (Scott et al., 2008a) while concomitantly reducing gill permeability to ions. Therefore, our second prediction was that a similar mechanism would occur in hypoxia-exposed killifish. Specifically, we posited that ionocyte surface area would be reduced through a decrease in exposed ionocyte density and/or by PVCs stretching over ionocytes, thereby decreasing their exposed surface. Contrary to our prediction, hypoxia exposure in FW and SW did not change the fractional surface area of the filaments occupied by exposed ionocytes (Fig. 10E). However, individual ionocyte surface area increased in 11 ppt fish in hypoxia (Fig. 10A). This is in accord with increased gill fluxes and paracellular permeability seen in 11-ppt acclimated fish (discussed earlier). We also observed an increase in PVC surface area in FW- and SW-fish , with hypoxia exposure, that could be explained by the PVCs increasing in size and spreading so as to cover up the ionocytes. This would be similar to the mechanism previously seen in oscar exposed to hypoxia (Matey et al., 2008; Wood et al., 2009; Matey et al., 2011). Overall, fish exposed to hypoxia show a less complex PVC surface, where contrary to normoxic fish, the well defined microridge structure disappeared.

The lower microridge density in hypoxia-exposed FW-fish (Fig. 10D) is in accord with this idea.

Conclusions

As the prevalence and severity of hypoxia in the world's aquatic environments increase, a comprehensive understanding of the physiological responses to hypoxia has become extremely important. Collectively, the present data elucidate the nature of the osmorespiratory compromise following acute hypoxia exposure in *Fundulus heteroclitus* at different salinities. Salinity had a strong influence on how killifish responded to hypoxia as measured by a wide range of parameters. This was in general accord with our overall hypothesis of a trade-off between efficient gas exchange and ion/water balance at the gills that is flexible and dependent on salinity and oxygen levels. Our results show that both FW- and SW-killifish are similar to the Amazonian oscar model of response to hypoxia, inasmuch as active and passive components of gill Na^+ transport were reduced, along with a decrease in water flux rates, pointing to an overall reduction in gill transcellular and paracellular permeability, particularly in FW, so that ionoregulatory homeostasis can be decoupled from the needs of respiratory gas exchange. In contrast, 11 ppt acclimated fish increased both Na^+ influx and efflux rates in hypoxia, as well as paracellular permeability, responses that follow the predictions for the classical osmorespiratory compromise. Since, hypothetically, osmotic gradients are minimal at the isosmotic point, this increase in gill permeability should not be of great physiological concern. These results complement our previous study (Giacomin et al., 2019), which demonstated that the greatest respiratory challenges for killifish during hypoxia occur in FW, and the least at the isosmotic salinity (11 ppt). Future studies should examine how these adjustments in gill permeability are achieved at cellular and molecular levels.

Acknowledgments

We thank Derrick Horne, Garnet Martens and Miki Fujita of the UBC Bioimaging Facility for skillful assistance with sample preparation and SEM imaging. The authors would like to thank both reviewers whose comments have greatly improved our manuscript.

Funding

Supported by Natural Sciences and Engineering Research Council of Canada (NSERC) Discovery Grants to CMW (RGPIN-2017-03843, RGPIN/473-2012) and PMS (RGPIN-203189). MG was supported by a 4-year graduate fellowship from the University of British Columbia.

Competing Interests

No competing interests declared.

Author Contributions

MG, PMS, and CMW designed the study, MG and JOO performed the experiments and data analyses, CMW and PMS obtained funding, MG wrote the first draft of the manuscript, and all co-authors edited it.

List of Abbreviations

$^{3}H_2O$	tritiated (radiolabeled) water
[^{3}H]PEG-4000	tritium-labeled polyethylene glycol, MW = 4000
ANOVA	analysis of variance
ATP	adenosine-5'-triphosphate
CR	clearance rate
DR	drinking rate
FSA	fractional surface area
FW	fresh water
HCT	hematocrit
J^{Na+} influx	unidirectional sodium influx rate
J^{Na+} efflux	unidirectional sodium efflux rate
$\dot{M}O_2$	oxygen consumption rate
PO_2	partial pressure of oxygen
ppt	parts per thousand (measurement of salinity)
PVC	pavement cell
SW	sea water
TEP	transepithelial potential

Literature Cited

Bergmeyer, H. U. (1983). *Methods of enzymatic analysis*. New York: Academic Press.

Blanchard, J. and Grosell, M. (2006). Copper toxicity across salinities from freshwater to seawater in the euryhaline fish *Fundulus heteroclitus*: is copper an ionoregulatory toxicant in high salinities? *Aquat. Toxicol.* **80**, 131–139.

Booth, J. H. (1978). The distribution of blood flow in the gills of fish: application of a new technique to rainbow trout (*Salmo gairdneri*). *J. Exp. Biol.* **73**, 119–129.

Boutilier, R. G. and St-Pierre, J. (2000). Surviving hypoxia without really dying. *Comp. Biochem. Physiol. A* **126**, 481–490.

Breves, J. P., Inokuchi, M., Yamaguchi, Y., Seale, A. P., Hunt, B. L., Watanabe, S., Lerner, D. T., Kaneko, T. and Grau, G. E. (2016). Hormonal regulation of aquaporin 3: opposing actions of prolactin and cortison in tilapia gill. *J. Endocrinol.* **230**, 325–337.

Cochran, R. E. and Burnett, L. E. (1996). Respiratory responses of the salt marsh animals *Fundulus heteroclitus*, *Leiostomus xanturus*, and *Palaemonetes pugio* to environmental hypoxia and hypercapnia and to the organophosphate pesticide, azinphosmethyl. *J. Exp. Mar. Bio. Ecol.* **195**, 125–144.

Cutler, C. P., Martinez, A.-S. and Cramb, G. (2007). The role of aquaporin 3 in teleost fish. *Comp. Biochem. Physiol. - A* **148**, 82–91.

De Boeck, G., Wood, C. M., Iftikar, F. I., Matey, V., Scott, G. R., Sloman, K. A., Paula da Silva, N. M., Almeida-Val, V. M. F. and Val, A. L. (2013). Interactions between hypoxia tolerance and food deprivation in Amazonian oscars, *Astronotus ocellatus*. *J. Exp. Biol.* **216**, 4590–4600.

Evans, D. H. (1969). Studies on the permeability to water of selected marine, freshwater and euryhaline teleosts. *J. Exp. Biol.* **50**, 689–703.

Evans, D. H. (2005). The multifunctional fish gill: dominant site of gas exchange, osmoregulation, acid-base regulation, and excretion of nitrogenous waste. *Physiol. Rev.* **85**, 97–177.

Evans, D. H. (2008). Teleost fish osmoregulation: what have we learned since August Krogh, Homer Smith, and Ancel Keys. *Am. J. Physiol. - Regul. Integr. Comp. Physiol.* **295**, R704–R713.

Farmer, G. J. and Beamish, F. W. H. (1969). Oxygen consumption of *Tilapia nilotica* in relation to swimming speed and salinity. *J Fish Board of Canada* **26,** 2807-2821.

Forgac, M. (1989). Structure and function of vacuolar class of ATP-driven proton pumps.

Physiological Reviews **69,** 765-796.

Giacomin, M., Schulte, P. M. and Wood, C. M. (2017). Differential effects of temperature on oxygen consumption and branchial fluxes of urea, ammonia, and water in the dogfish shark (*Squalus acanthias suckleyi*). *Physiol. Biochem. Zool.* **90**, 694296.

Giacomin, M., Bryant, H. J., Val, A. L., Schulte, P. M. and Wood, C. M. (2019). The osmorespiratory compromise: physiological responses and tolerance to hypoxia are affected by salinity acclimation in the euryhaline Atlantic killifish (*Fundulus heteroclitus*). *J. Exp. Biol.* **222,** jeb206599.

Gonzalez, R. J. (2011). Role of the gills: the osmorespiratory compromise. In *Encyclopedia of Fish Physiology* (ed. Farrell, A. P.), pp. 1389–1394. Elsevier Inc.

Gonzalez, R. J. and McDonald, D. G. (1992). The relationship between oxygen consumption and ion loss in a freshwater fish. *J. Exp. Biol.* **163**, 317–332.

Gonzalez, R. J. and McDonald, D. G. (1994). The relationship between oxygen uptake and ion loss in fish from diverse habitats. *J. Exp. Biol.* **190**, 95–108.

Healy, T. M. and Schulte, P. M. (2012). Thermal acclimation is not necessary to maintain a wide thermal breadth of aerobic scope in the common killifish (*Fundulus heteroclitus*). *Physiol. Biochem. Zool.* **85**, 107–119.

Hochachka, P. W., Buck, L. T., Doll, C. J. and Land, S. C. (1996). Unifying theory of hypoxia tolerance: molecular/metabolic defense and rescue mechanisms for surviving oxygen lack. *Proc. Natl. Acad. Sci.* **93**, 9493–9498.

Hofmann, E. L. and Butler, D. G. (1979). The effect of increased metabolic rate on renal function in the rainbow trout, *Salmo gairdneri*. *J. Exp. Biol.* **82**, 11–23.

Holmes, W. N. and Donaldson, E. M. (1969). The body compartments and the distribution of electrolytes. In *Fish Physiology Vol. 1* (eds. Hoar, W. S. and Randall, D. J.), pp. 1–89. New York, NY: Academic Press.

Iftikar, F. I., Matey, V. and Wood, C. M. (2010). The ionoregulatory responses to hypoxia in the freshwater rainbow trout *Oncorhynchus mykiss*. *Physiol. Biochem. Zool.* **83**, 343–355.

Isaia, J. (1984). Water and nonelectrolyte permeation. In *Fish Physiology, Vol. 10B* (eds. Hoar, W. S. and Randall, D. J.), pp. 1–38. San Diego, CA: Academic Press.

Katoh, F. and Kaneko, T. (2002). Effects of environmental Ca^{2+} levels on branchial chloride cell morphology in freshwater-adapted killifish Fundulus heteroclitus. *Scan. Electron Microsc.* 347–355.

Katoh, F. and Kaneko, T. (2003). Short-term transformation and long-term replacement of

branchial chloride cells in killifish transferred from seawater to freshwater, revealed by morphofunctional observations and a newly established “time-differential double fluorescent staining” techniq. *J. Exp. Biol.* **206**, 4113–4123.

Laurén, D. J. and McDonald, D. G. (1985). Effects of copper on branchial ionoregulation in the rainbow trout, *Salmo gairdneri* Richardson. *J. Comp. Physiol. B* **155**, 635–644.

Layman, C. A., Smith, D. E. and Herod, J. D. (2000). Seasonally varying importance of abiotic and biotic factors in marsh-pond fish communities. *Mar. Ecol. Prog. Ser.* **207**, 155–169.

Lin, H. and Randall, D. J. (1993). H^+-ATPase activity in crude homogenates of fish gill tissue: inhibitor sensitivity and environmental and hormonal regulation. *J. Exp. Biol.* **180**, 163–174.

Loretz, A. C. (1979). Water exchange across fish gills: the significance of triated-water flux measurements. *J. Exp. Biol.* **79**, 147–162.

Madsen, S. S., Engelund, M. B. and Cutler, C. P. (2015). Water transport and functional dynamics of aquaporins in osmoregulatory organs of fishes. *Biol. Bull.* **229**, 70–92.

Maetz, J., Sawyer, W. H., Pickford, G. E. and Mayer, N. (1967). Evolution de la balance minérale du sodium chez *Fundulus heteroclitus*au cours du transfert d’eau de mer en eau douce: effets de l’hypophysectomie et de la prolactine. *Gen. Comp. Endocrinol.* **8**, 163–176.

Malvin, R. L., Schiff, D. and Eiger, S. (1980). Angiotensin and drinking rates in the euryhaline killifish. *Am. J. Physiol. Integr. Comp. Physiol.* **239**, R31–R34.

Marshall, W. S. (2013). Osmoregulation in estuarine and intertidal fishes. In *Fish Physiology, Vol. 32* (eds. McCormick, S. D., Farrell, A. P., and Brauner, C. J.), pp. 395–434. New York: Academic Press.

Matey, V., Richards, J. G., Wang, Y., Wood, C. M., Rogers, J., Davies, R., Murray, B. W., Chen, X.-Q., Du, J. and Brauner, C. J. (2008). The effect of hypoxia on gill morphology and ionoregulatory status in the Lake Qinghai scaleless carp, *Gymnocypris przewalskii*. *J. Exp. Biol.* **211**, 1063–1074.

Matey, V., Iftikar, F. I., De Boeck, G., Scott, G. R., Sloman, K. A., Almeida-Val, V. M. F., Val, A. L. and Wood, C. M. (2011). Gill morphology and acute hypoxia: responses of mitochondria-rich, pavement, and mucous cells in the Amazonian oscar (*Astronotus ocellatus*) and the rainbow trout (*Oncorhynchus mykiss*), two species with very different approaches to the osmo-r. *Can. J. Zool.* **89**, 307–324.

McCormick, S. D. (1993). Methods for nonlethal gill biopsy and measurement of Na^+, K^+-

ATPase activity. *Can. J. Fish. Aquat. Sci.* **50**, 656–658.

Milligan, C. L. and Wood, C. M. (1986). Tissue intracellular acid-base status and the fate of lactate after exhaustive exercise in the rainbow trout. *J. Exp. Biol.* **123**, 123–144.

Motais, R., Romeu, F. G. and Maetz, J. (1966). Exchange diffusion effect and euryhalinity in teleosts. *J. Gen. Physiol.* **50**, 391–422.

Nilsson, G., Löfman, C. O. and Block, M. (1995). Extensive erythrocyte deformation in fish gills observed by in vivo microscopy: apparent adaptations for enhancing oxygen uptake. *J. Exp. Biol.* **198**, 1151–1156.

Olson, K. R. (1992). Blood and extracellular fluid volume regulation: role of the renin-angiotensin system, kallikrein-kinin system, and atrial natriuretic peptides. In *Fish Physiology Vol. 12B* (eds. Hoar, W. S., Randall, D. J., and Farrell, A. P.), pp. 135–254. San Diego, CA: Academic Press.

Onukwufor, J. O. and Wood, C. M. (2018). The osmorespiratory compromise in rainbow trout (*Oncorhynchus mykiss*): the effects of fish size, hypoxia, temperature and strenuous exercise on gill diffusive water fluxes and sodium net loss rates. *Comp. Biochem. Physiol. A* **219**–**220**, 10–18.

Patrick, M. L. and Wood, C. M. (1999). Ion and acid-base regulation in the freshwater mummichog (*Fundulus heteroclitus*): A departure from the standard model for freshwater teleosts. *Comp. Biochem. Physiol. A* **122**, 445–456.

Patrick, M. L., Part, P., Marshall, W. S. and Wood, C. M. (1997). Characterization of ion and acid-base transport in the fresh water adapted mummichog (*Fundulus heteroclitus*). *J. Exp. Zool.* **279**, 208–219.

Perry, S. F., Jonz, M. G. and Gilmour, K. M. (2009). Oxygen sensing and the hypoxic ventilatory response. In *Fish Physiology* (eds. Farrell, A. P., Brauner, C. J., and Richards, J. G.), pp. 193–253. San Diego, CA: Academic Press.

Postlethwaite, E. K. and McDonald, D. G. (1995). Mechanisms of Na^+ and Cl^- regulation in freshwater-adapted rainbow trout (*Oncorhynchus mykiss*) during exercise and stress. *J. Exp. Biol.* **198**, 295–304.

Potts, W. T. W. and Evans, D. H. (1967). Sodium and chloride balance in the killifish *Fundulus heteroclitus*. *Biol. Bull.* **133**, 411–425.

Potts, W. T. W. and Fleming, W. R. (1970). The effects of prolactin and divalent ions on the permeability to water of *Fundulus kansae*. *J. Exp. Biol.* **53**, 317–327.

Randall, D. J., Baumgarten, D. and Malyusz, M. (1972). The relationship between gas and ion transfer across the gills of fishes. *Comp. Biochem. Physiol. A* **41**, 629–637.

Richards, J. G., Wang, Y. S., Brauner, C. J., Gonzalez, R. J., Patrick, M. L., Schulte, P. M., Choppari-Gomes, A. R., Almeida-Val, V. M. and Val, A. L. (2007). Metabolic and ionoregulatory responses of the Amazonian cichlid, *Astronotus ocellatus*, to severe hypoxia. *J. Comp. Physiol. B* **177**, 361–374.

Richards, J. G., Sardella, B. A. and Schulte, P. M. (2008). Regulation of pyruvate dehydrogenase in the common killifish, *Fundulus heteroclitus*, during hypoxia exposure. *Am. J. Physiol. Integr. Comp. Physiol.* **295**, R979–R990.

Robertson, L. M. and Wood, C. M. (2014). Measuring gill paracellular permeability with polyethylene glycol-4000 in freely swimming trout: proof of principle. *J. Exp. Biol.* **217**, 1425–1429.

Robertson, L. M., Kochhann, D., Bianchini, A., Matey, V., Almeida-Val, V. M. F., Val, A. L. and Wood, C. M. (2015a). Gill paracellular permeability and the osmorespiratory compromise during exercise in the hypoxia tolerant Amazonian oscar (*Astronotus ocellatus*). *J. Comp. Physiol. B* **185**, 741–754.

Robertson, L. M., Val, A. L., Almeida-Val, V. F. and Wood, C. M. (2015b). Ionoregulatory aspects of the osmorespiratory compromise during acute environmental hypoxia in 12 tropical and temperate teleosts. *Physiol. Biochem. Zool.* **88**, 357–370.

Sardella, B. A. and Brauner, C. J. (2007). The Osmo-respiratory Compromise in Fish: The Effects of Physiological State and the Environment. In *Fish Respiration and Environment* (eds. Fernandes, M. N., Rantin, F. T., Glass, M. L., and Kapoor, B. G.), pp. 147–165. Enfield, NH: Science Publishers.

Scott, G. R., Schulte, P. M. and Wood, C. M. (2006). Plasticity of osmoregulatory function in the killifish intestine: drinking rates, salt and water transport, and gene expression after freshwater transfer. *J. Exp. Biol.* **209**, 4040–4050.

Scott, G. R., Wood, C. M., Sloman, K. A., Iftikar, F. I., De Boeck, G., Almeida-Val, V. M. F. and Val, A. L. (2008a). Respiratory responses to progressive hypoxia in the Amazonian oscar, *Astronotus ocellatus*. *Respir. Physiol. Neurobiol.* **162**, 109–116.

Scott, G. R., Baker, D. W., Schulte, P. M. and Wood, C. M. (2008b). Physiological and molecular mechanisms of osmoregulatory plasticity in killifish after seawater transfer. *J. Exp. Biol.* **211**, 2450–2459.

Smith, K. J. and Able, K. W. (2003). Dissolved oxygen dynamics in salt marsh pools and its potential impacts on fish assemblages. *Mar. Ecol. Prog. Ser.* **258**, 223–232.

Stevens, E. D. (1972). Change in body weight caused by handling and exercise in fish. *J. Fish Board of Canada* **29**, 202–203.

Sundin, L. and Nilsson, G. E. (1998). Endothelin redistributes blood flow through the lamellae of rainbow trout gills. *J. Comp. Physiol. B* **168**, 619–623.

Takei, Y. and Balment, R. J. (2009). The neuroendocrine regulation of fluid intake and fluid balance. In *Fish Physiology Vol. 28* (eds. Bernier, N. J., Van Der Kraak, G., Farrell, A. P., and Brauner, C. J.), pp. 365–419. San Diego, CA: Academic Press.

Thomas, S., Fievet, B. and Motais, R. (1986). Effect of deep hypoxia on acid-base balance in trout: role of ion transfer processes. *Am. J. Physiol.* **250**, R319–R327.

Tipsmark, C. K., Madsen, S. S. and Borski, R. J. (2004). Effect of salinity on expression of branchial ion transporters in striped bass (*Morone saxatilis*). *J. Exp. Zool.* **301**, 979–991.

Verdouw, H., van Echteld, C. J. A. and Dekkers, E. M. J. (1978). Ammonia determination based on indophenol formation with sodium salicylate. *Water Res.* **12**, 399–402.

Weihrauch, D., Wilkie, M. P. and Walsh, P. J. (2009). Ammonia and urea transporters in gills of fish and aquatic crustaceans. *J. Exp. Biol.* **212**, 1716–1730.

Wilkie, M. P. (1997). Mechanisms of ammonia excretion across fish gills. *Comp. Biochem. Physiol. A* **118**, 39–50.

Wilkie, M. P. (2002). Ammonia excretion and urea handling by fish gills: Present understanding and future research challenges. *J. Exp. Zool.* **293**, 284–301.

Wood, C. M. (2011). Rapid regulation of Na^+ and Cl^- flux rates in killifish after acute salinity challenge. *J. Exp. Mar. Bio. Ecol.* **409**, 62–69.

Wood, C. M. and Laurent, P. (2003). Na^+ versus Cl^- transport in the intact killifish after rapid salinity transfer. *Biochim. Biophys. Acta* **1618**, 106–119.

Wood, C. M. and Marshall, W. S. (1994). Ion balance, acid-base regulation, and chloride cell function in the common killifish, *Fundulus heteroclitus* - a euryhaline estuarine teleost. *Estuaries* **17**, 34–52.

Wood, C. M. and Part, P. (1997). Cultured branchial epithelia from freshwater fish gills. *J. Exp. Biol.* **200**, 1047–1059.

Wood, C. M. and Randall, D. J. (1973a). The influence of swimming activity on sodium balance in the rainbow trout (*Salmo gairdneri*). *J. Comp. Physiol.* **82**, 207–233.

Wood, C. M. and Randall, D. J. (1973b). Sodium balance in the rainbow trout (*Salmo gairdneri*) during extended exercise. *J. Comp. Physiol.* **82**, 235–256.

Wood, C. M. and Randall, D. J. (1973c). The influence of swimming activity on water balance in the rainbow trout (*Salmo gairdneri*). *J. Comp. Physiol.* **82**, 257–276.

Wood, C. M., Kajimura, M., Sloman, K. A., Scott, G. R., Walsh, P. J., Almeida-Val, V.

M. F. and Val, A. L. (2007). Rapid regulation of Na^+ fluxes and ammonia excretion in response to acute environmental hypoxia in the Amazonian oscar, *Astronotus ocellatus*. *Am. J. Physiol. Regul. Integr. Comp. Physiol.* **292**, R2048–R2058.

Wood, C. M., Iftikar, F. I., Scott, G. R., De Boeck, G., Sloman, K. A., Matey, V., Valdez Domingos, F. X., Duarte, R. M., Almeida-Val, V. M. F. and Val, A. L. (2009). Regulation of gill transcellular permeability and renal function during acute hypoxia in the Amazonian oscar (*Astronotus ocellatus*): new angles to the osmorespiratory compromise. *J. Exp. Biol.* **212**, 1949–1964.

Wood, C.M., Ruhr I.M., Schauer, K.L., Y. Wang, Mager, E.M., McDonald, D., Stanton, B., and Grosell, M. (2019). The osmorespiratory compromise in the euryhaline killifish: water regulation during hypoxia. *J. Exp. Biol***. *222,*** jeb204818

Wright, P. A. and Wood, C. M. (2009). A new paradigm for ammonia excretion in aquatic animals: role of Rhesus (Rh) glycoproteins. *J. Exp. Biol.* **212**, 2303–2312.

Zall, D. M., Fisher, D. and Garner, M. Q. (1956). Photometric determination of chlorides in water. *Anal. Chem.* **28**, 1665–1668.

Figures

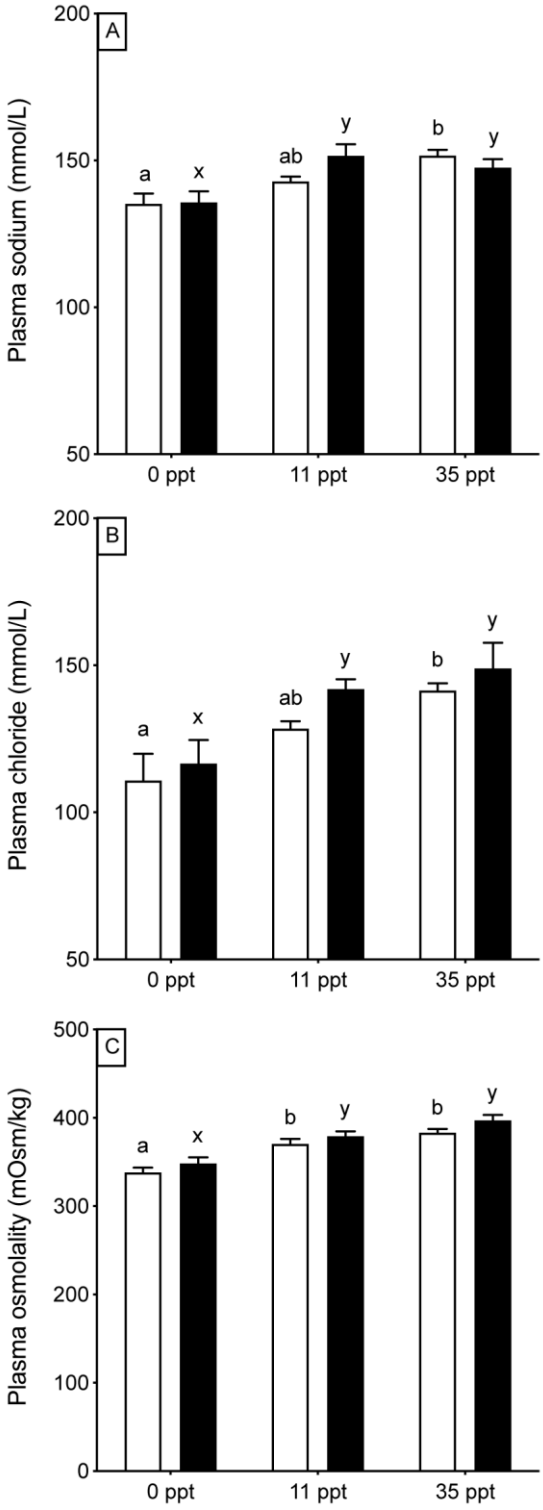

Figure 1. (A) Plasma sodium (mmol/L), (B) plasma chloride (mmol/L) and (C) plasma osmolality (mOsm/kg) in *Fundulus heteroclitus* acclimated to 0, 11 and 35 ppt in normoxia (white bars) and exposed to hypoxia (black bars). Bars sharing the same lower case letters are not statistically different at the same oxygen level. [Two-way ANOVA p-values (**plasma Na^+:** $p_{interaction}$= .1221, p_{oxygen}= .5051, $p_{salinity}$< .0001; **plasma Cl^-:** $p_{interaction}$= .8137, p_{oxygen}= .0909, $p_{salinity}$< .0001; **plasma osmolality:** $p_{interaction}$= .8878, p_{oxygen}= .0217, $p_{salinity}$< .0001)]. Means ± SEM (n = 8).

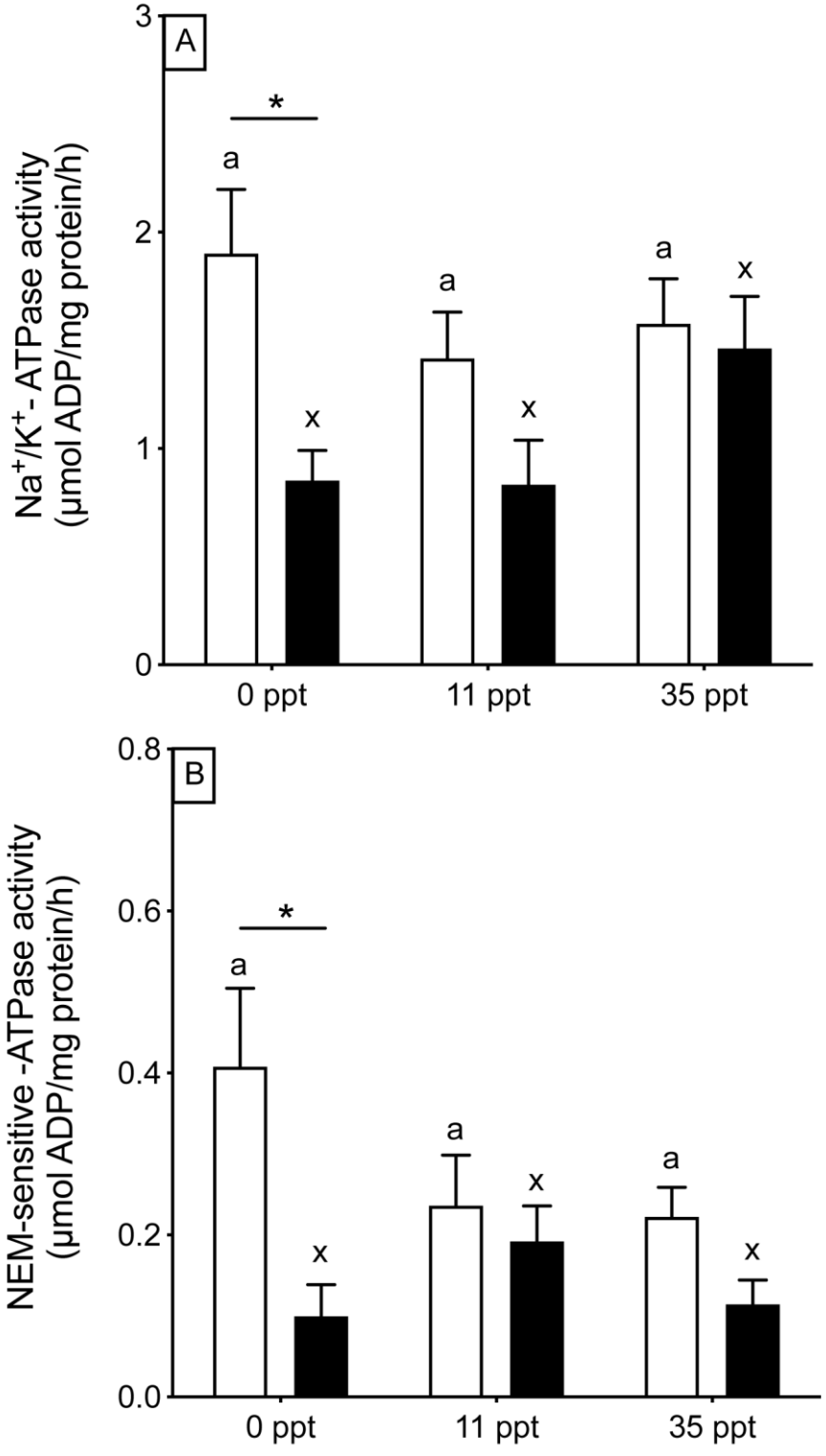

Figure 2. (A) Na^+/K^+-ATPase and (B) NEM-sensitive -ATPase activity (µmol ADP/mg protein/h) in *Fundulus heteroclitus* acclimated to 0, 11 and 35 ppt in normoxia (white bars) and exposed to hypoxia (black bars). Bars sharing the same lower case letters are not statistically different at the same oxygen level. [Two-way ANOVA p-values (**Na^+/K^+-ATPase:** $p_{interaction}$= .1356, p_{oxygen}= .0037, $p_{salinity}$= .2233; **NEM-sensitive -ATPase:** $p_{interaction}$= .0608, p_{oxygen}= .0011, $p_{salinity}$= .2622)]. Asterisks indicate significant differences between normoxia and hypoxia at the same salinity (Bonferroni post-hoc test). Means ± SEM (n = 8).

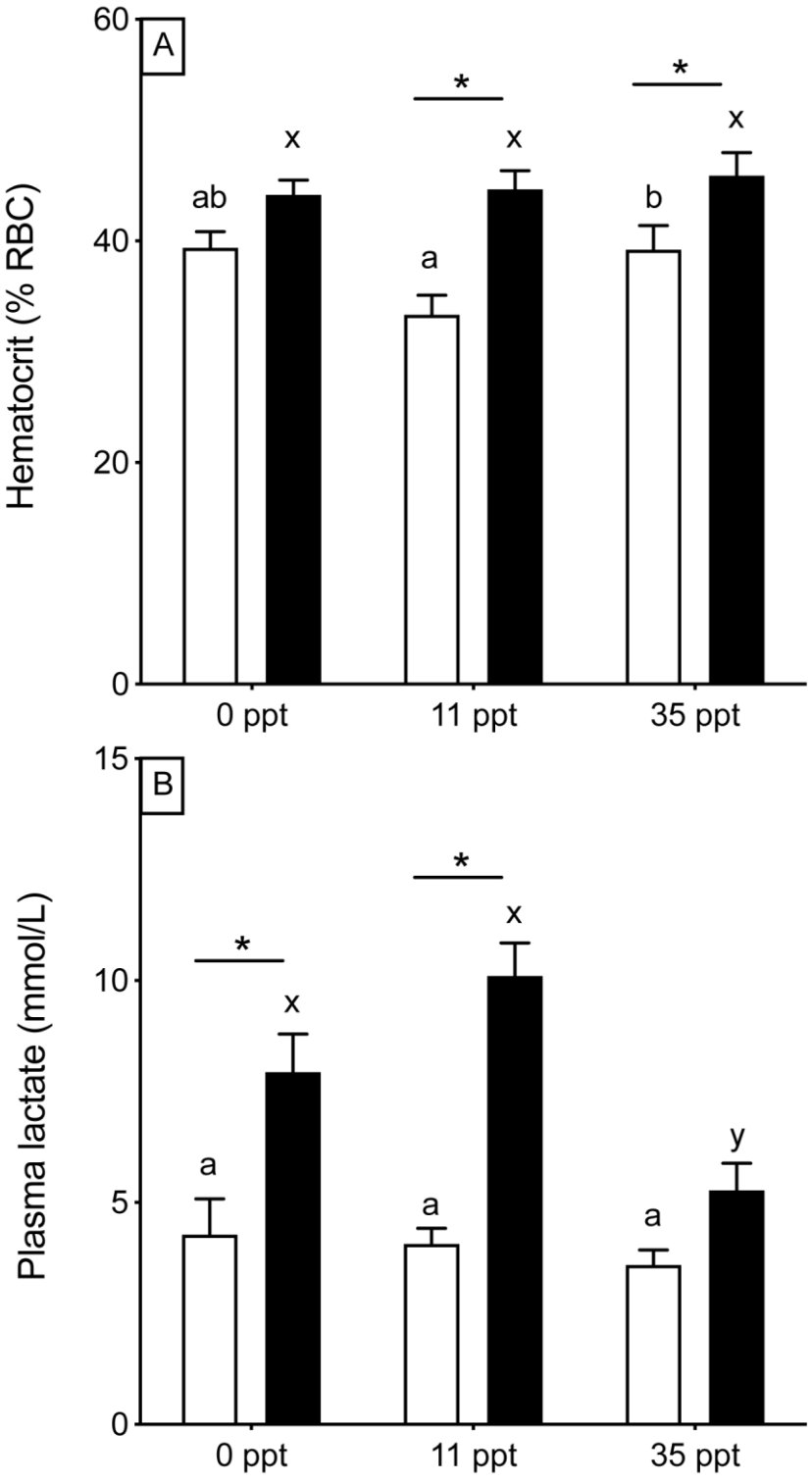

Figure 3. (A) Hematocrit (% RBC) and (B) plasma lactate (mmol/L) in *Fundulus heteroclitus* acclimated to 0, 11 and 35 ppt in normoxia (white bars) and exposed to hypoxia (black bars). Bars sharing the same lower case letters are not statistically different at the same oxygen

level. [Two-way ANOVA p-values (**hematocrit:** $p_{interaction}$= .1845, p_{oxygen}< .0001, $p_{salinity}$= .1239; **lactate:** $p_{interaction}$= .0051, p_{oxygen}< .0001, $p_{salinity}$= .0006)]. Asterisks indicate significant differences between normoxia and hypoxia at the same salinity (Bonferroni post-hoc test). Means ± SEM (n = 8).

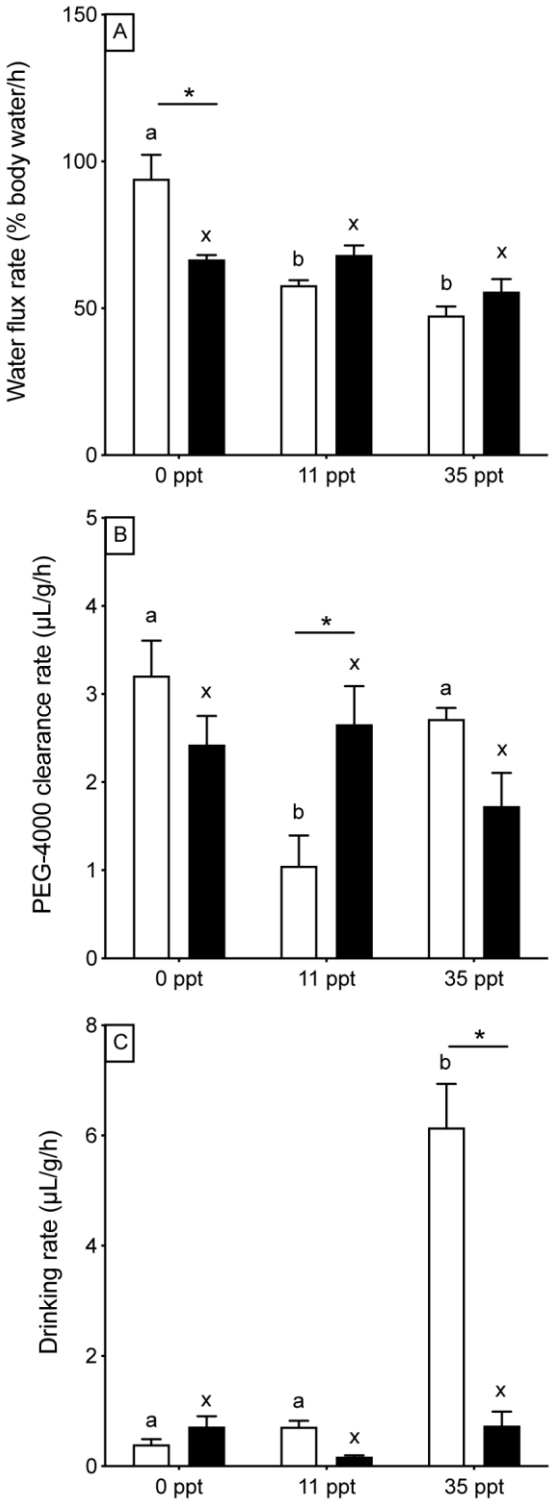

Figure 4. (A) Water flux rate (% body water/h) (B) PEG-4000 clearance rate (µL/g/h) and (C) drinking rate (µL/g/h) in *Fundulus heteroclitus* acclimated to 0, 11 and 35 ppt in normoxia (white bars) and exposed to hypoxia (black bars). Bars sharing the same lower case letters are not statistically different at the same oxygen level. [Two-way ANOVA p-values

(**water flux rate:** $p_{interaction} < .0001$, $p_{oxygen} = .3608$, $p_{salinity} < .0001$; **clearance rate:** $p_{interaction} = .0046$, $p_{oxygen} = .8712$, $p_{salinity} = .03733$; **drinking rate:** $p_{interaction} < .0001$, $p_{oxygen} < .0001$, $p_{salinity} < .0001$]. Asterisks indicate significant differences between normoxia and hypoxia at the same salinity (Bonferroni post-hoc test). Means ± SEM (n = 12 for [A] and n = 8 for [B,C]).

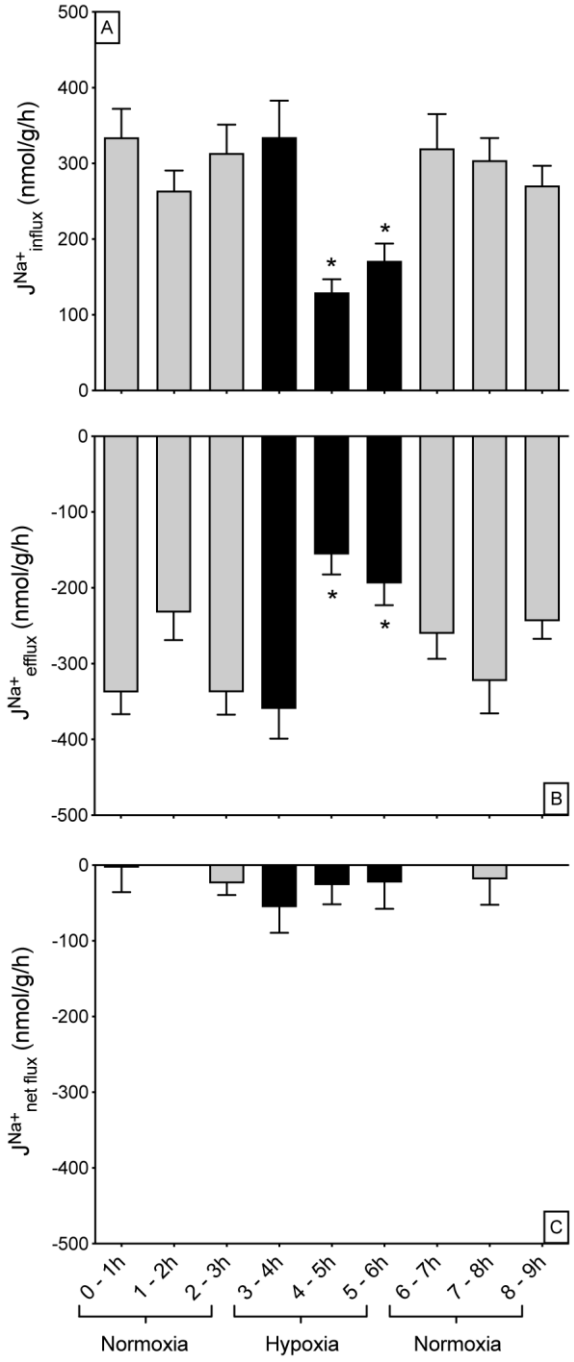

Figure 5. (A) Unidirectional sodium influx rate (J^{Na+}_{influx}; nmol/g/h), (B) unidirectional sodium efflux rate (J^{Na+}_{efflux}; nmol/g/h) and (C) sodium net flux ($J^{Na+}_{net\ flux}$; nmol/g/h) rate in *Fundulus heteroclitus* acclimated to 0 ppt. Fish were subjected to 3 h each of normoxia, hypoxia, and normoxia. Asterisks indicate bars which are significantly different from the averaged starting normoxia period (Dunnett's test). Data are means ± SEM (n = 15).

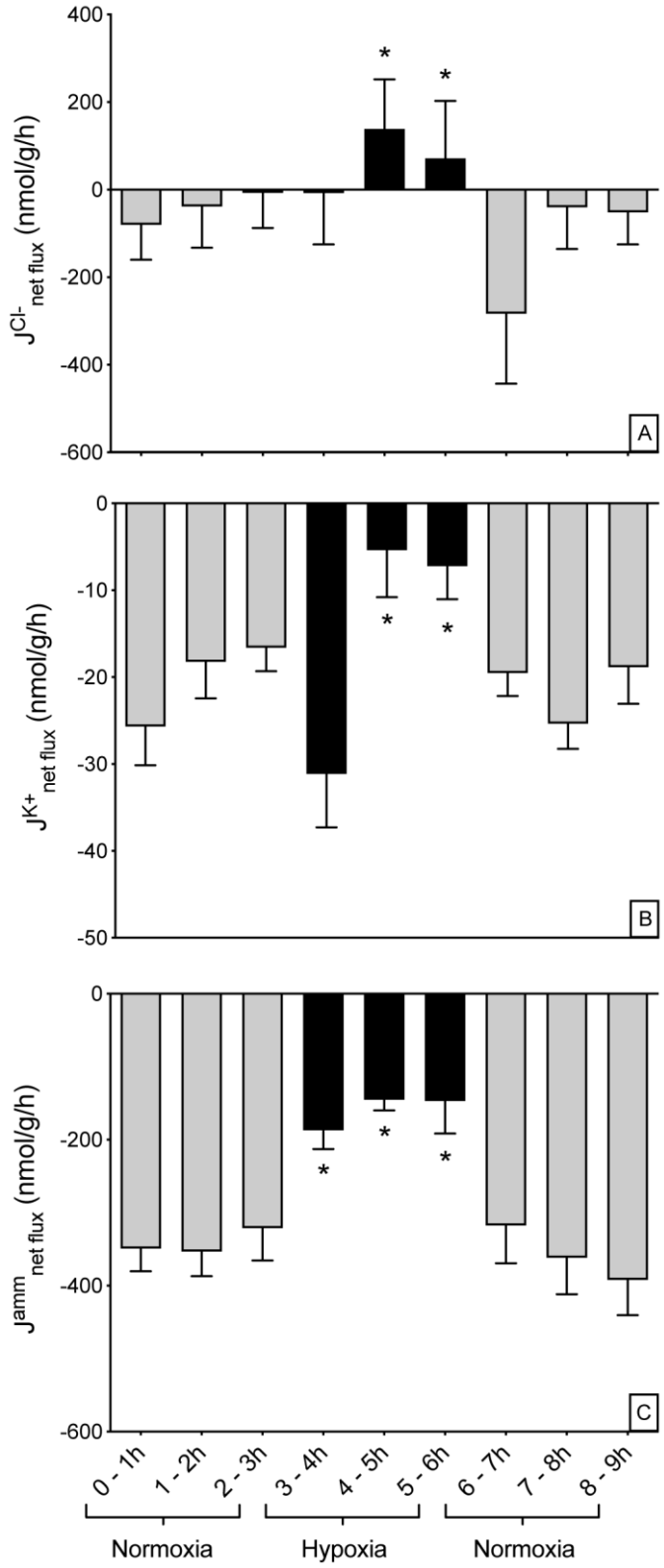

Figure 6. The effect of hypoxia exposure on the (A) chloride net flux rate ($J^{Cl-}_{net\ flux}$; nmol/g/h), (B) potassium net flux rate ($J^{K+}_{net\ flux}$; nmol/g/h) and (C) ammonia net flux rate ($J^{amm}_{net\ flux}$; nmol/g/h) in *Fundulus heteroclitus* acclimated to 0 ppt. Fish were subjected to 3 h each of normoxia, hypoxia, normoxia. Asterisks indicate bars which are significantly different from the averaged starting normoxia period (Dunnett's test). Means ± SEM (n = 15).

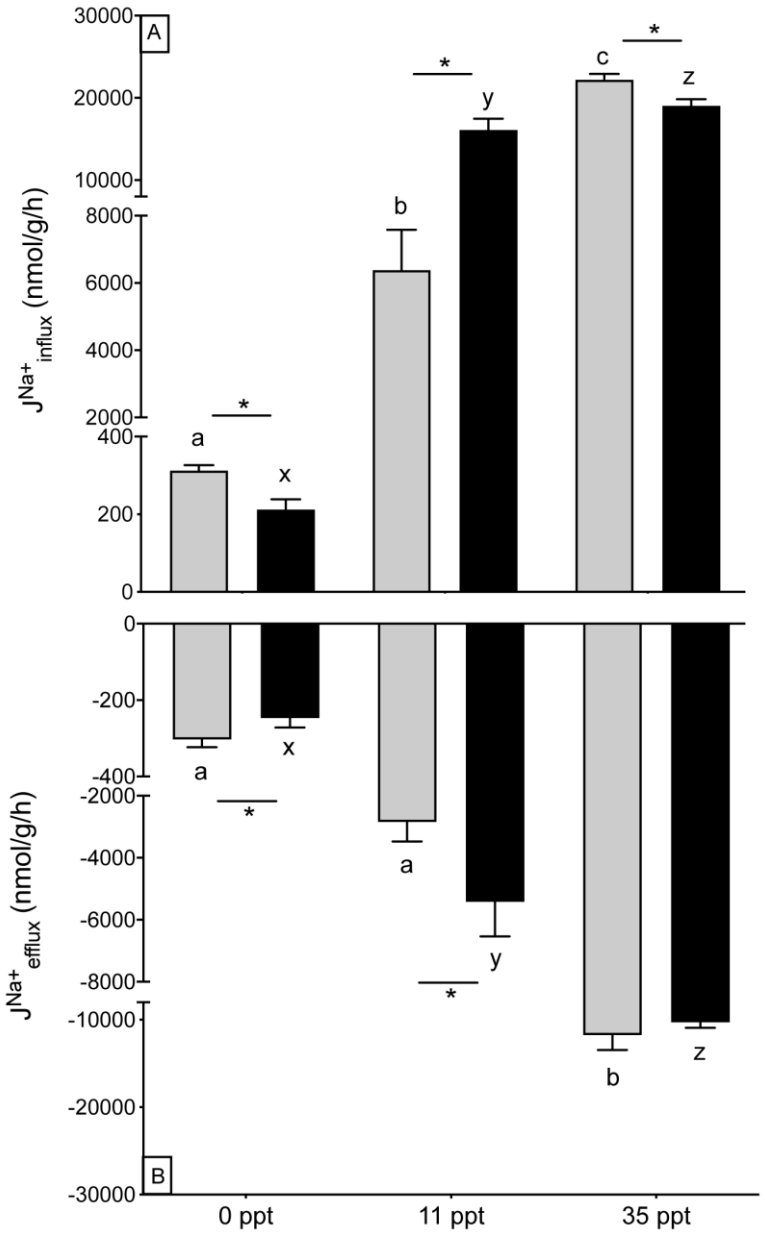

Figure 7. (A) unidirectional sodium influx rate (J^{Na+}_{influx}; nmol/g/h) and (B) unidirectional sodium efflux rate (J^{Na+}_{efflux}; nmol/g/h) in *Fundulus heteroclitus* acclimated to 0 ppt, 11 ppt and 35 ppt in normoxia (grey bars) and exposed to hypoxia (black bars). 0 ppt data are averaged data from Fig. 5. Bars sharing the same lower case letters are not statistically different at the same oxygen level. [Two-way ANOVA p-values ($\mathbf{J^{Na+}_{influx}}$**:** $p_{interaction} < .0001$, $p_{oxygen} = .0004$, $p_{salinity} < .0001$; $\mathbf{J^{Na+}_{efflux}}$**:** $p_{interaction} = .1059$, $p_{oxygen} = .6178$, $p_{salinity} < .0001$)]. Asterisks indicate significant differences between normoxia and hypoxia at the same salinity (Bonferroni post-hoc test). Means ± SEM (n = 15).

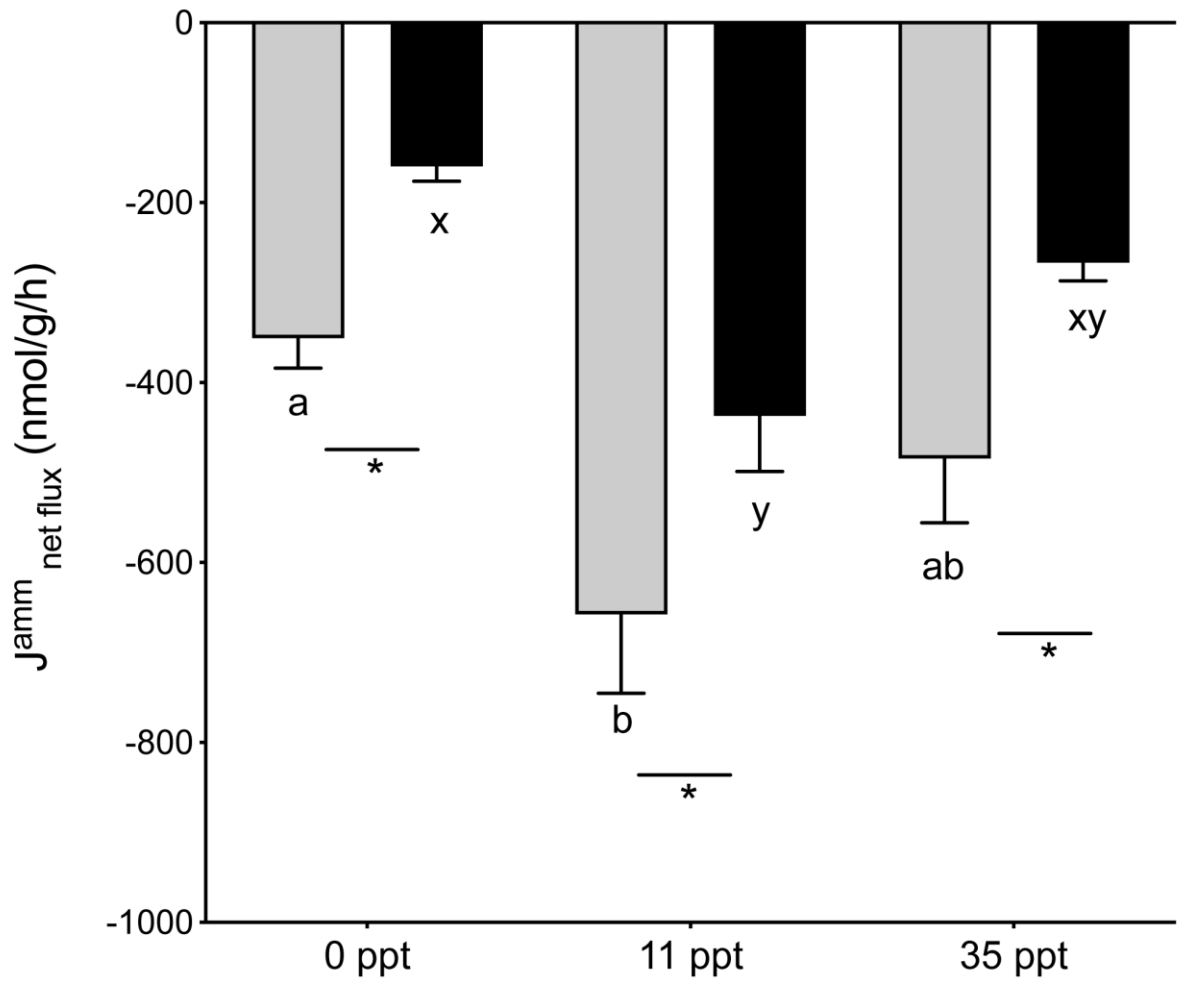

Figure 8. Ammonia net flux rate (J_{amm}; nmol/g/h) in *Fundulus heteroclitus* acclimated to 0 ppt, 11 ppt and 35 ppt in normoxia (grey bars) and exposed to hypoxia (black bars). 0 ppt data are averaged data from Fig. 6C. Bars sharing the same lower case letters are not statistically different at the same oxygen level. [Two-way ANOVA p-values ($\mathbf{J_{amm}}$**:** $p_{interaction}$=.9560, p_{oxygen}< .0001, $p_{salinity}$< .0001]. Asterisks indicate significant differences between normoxia and hypoxia at the same salinity (Bonferroni post-hoc test). Means ± SEM (n = 15).

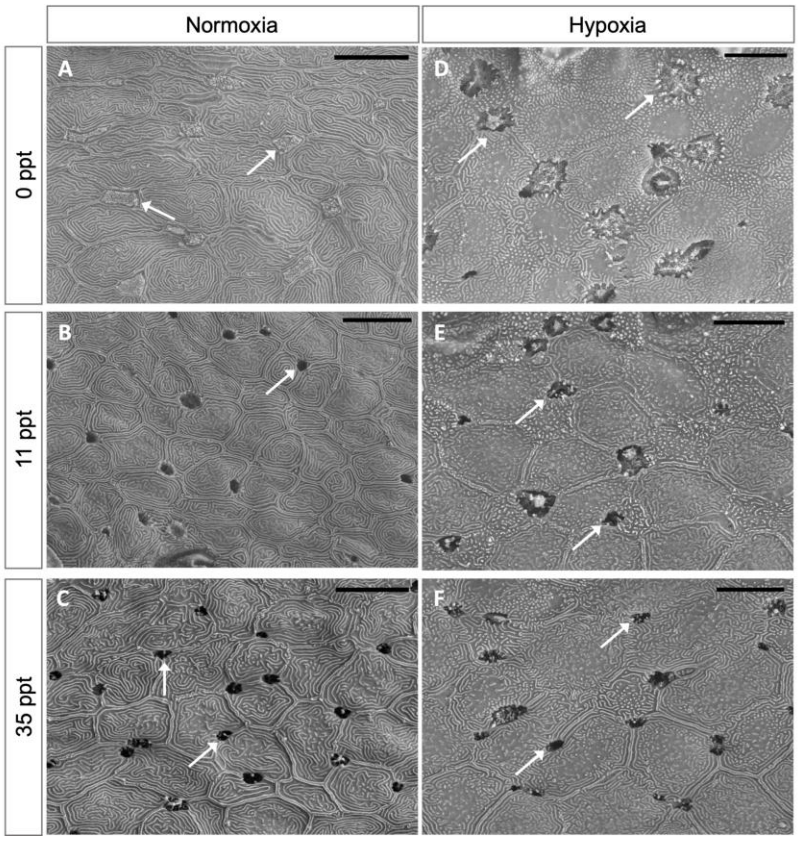

Figure 9. Representative scanning electron microscopy (SEM) images of gill filaments of of *Fundulus heteroclitus* acclimated to (A) 0 ppt (B) 11 ppt and (C) 35 ppt in normoxia and exposed to hypoxia for 3 h in (D) 0 ppt , (E) 11 ppt , and (F) 35 ppt. White arrows indicate ionocytes. Scale bars are 10 µm.

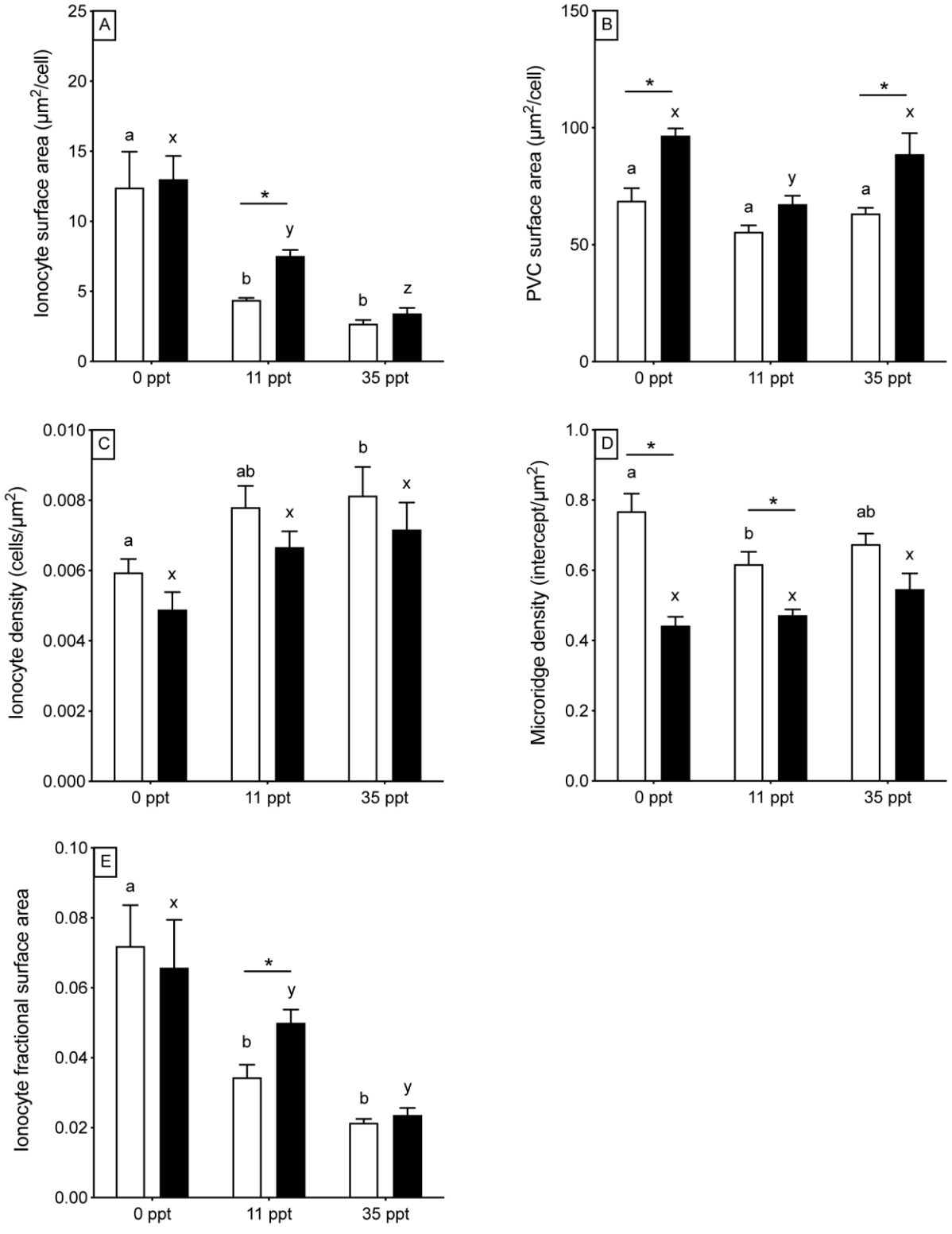

Figure 10. (A) Individual ionocyte surface area (μm^2/cell), (B) pavement cell (PVC) surface area (μm^2/cell), (C) ionocyte density (cells/μm^2), (D) PVC microridge density (intercepts/μm^2) and (E) ionocyte SA x density (i.e. fractional surface area) in *Fundulus heteroclitus* acclimated to 0, 11 and 35 ppt in normoxia (white bars) and exposed to hypoxia

(black bars). Bars sharing the same lower case letters are not statistically different at the same oxygen level. [Two-way ANOVA p-values (**ionocyte surface area:** $p_{interaction}$= .5202, p_{oxygen}= .0521, $p_{salinity}$< .0001; **PVC area:** $p_{interaction}$= .3175, p_{oxygen}= .0001, $p_{salinity}$= .0036; **ionocyte density:** $p_{interaction}$= .9903, p_{oxygen}= .0535, $p_{salinity}$= .0050; **microridge density:** $p_{interaction}$= .0275, p_{oxygen}< .0001, $p_{salinity}$= .1683; **ionocyte fractional SA:** $p_{interaction}$= .3634, p_{oxygen}= .5289, $p_{salinity}$< .0001)]. Asterisks indicate significant differences between normoxia and hypoxia at the same salinity (Bonferroni post-hoc test). Means ± SEM (n = 5).